

ORNL TECHNICAL INFORMATION
DIVISION
Y-12 TECHNICAL LIBRARY
Document Reference Section
LOAN COPY ONLY

OAK RIDGE NATIONAL LABORATORY LIBRARIES



3 4456 0599467 6

NUREG/CR-0778
(ORNL/Sub-2913/10)
Dist. Category R5

cy. 2



Do NOT transfer this document to any other person. If you want others to see it, attach their names, return the document, and the Library will arrange the loan as requested.

UCN-1624
(3 5-60)

STRESS INDICES AND FLEXIBILITY FACTORS FOR NOZZLES IN PRESSURE VESSELS AND PIPING

E. C. Rodabaugh
S. E. Moore

Work funded by
U.S. Nuclear Regulatory Commission
Office of Nuclear Regulatory Research
Under Interagency Agreements 40-551-75 and 40-552-75
NRC FIN No. B0123

June, 1979

Work Performed by

Battelle
Columbus Laboratories
505 King Avenue
Columbus, Ohio 43201

for
OAK RIDGE NATIONAL LABORATORY
Oak Ridge, Tennessee 37830
operated by
UNION CARBIDE CORPORATION
for the
DEPARTMENT OF ENERGY

Contract No. W-7405-eng-26

Printed in the United States of America
Available from
National Technical Information Service
U.S. Department of Commerce
5285 Port Royal Road
Springfield, Virginia 22151
Price: Printed Copy \$6.00; Microfiche \$3.00

This report was prepared as an account of work sponsored by the United States Government. Neither the United States nor the Energy Research and Development Administration, nor the Nuclear Regulatory Commission, nor any of their employees, nor any of their contractors, subcontractors, or their employees, makes any warranty, express or implied, or assumes any legal liability or responsibility for the accuracy, completeness or usefulness of any information, apparatus, product or process disclosed, or represents that its use would not infringe privately owned rights.

STRESS INDICES AND FLEXIBILITY FACTORS
FOR NOZZLES IN PRESSURE VESSELS AND PIPING

by

E. C. Rodabaugh
S. E. Moore

Manuscript Completed: May, 1979

Date Published: June, 1979

NOTICE This document contains information of a preliminary nature and was prepared primarily for internal use at the Oak Ridge National Laboratory. It is subject to revision or correction and therefore does not represent a final report.

Work funded by
U.S. Nuclear Regulatory Commission
Office of Nuclear Regulatory Research
Under Interagency Agreements 40-551-75 and 40-552-75
NRC FIN No. B0123

1

2

3

4

5

6

7

TABLE OF CONTENTS

	<u>Page</u>
FOREWORD	iii
ABSTRACT	vi
NOMENCLATURE	vii
1. INTRODUCTION	1
2. STRESS INDICES FOR PRESSURE	2
Introduction	2
Stress Indices for Relatively Simple Geometries	2
Stress Indices for Nozzles	4
Calculated Stresses	10
Test Data	12
Correlation Equations	13
Comparisons With Test Data	14
Photoelastic Test Data	14
Steel Models Test Data	15
Comparison with Reference (15) Finite Element Analysis	16
Influence of L_n in S-Type Models	16
Stress Indices for Nozzles Meeting Code Rules	17
S1-Type Nozzles	17
U2T-Type Nozzles	17
Recommendations for C_1 and K_1	19
3. STRESS INDICES FOR MOMENTS	21
Introduction	21
Stress Indices for Relatively Simple Geometries	21
Stress Indices for Nozzles	24
Moments on Nozzles	26
Moments Through Vessel	27
Recommendations for C_2 and K_2	28
4. FLEXIBILITY FACTORS	30
Introduction	30

TABLE OF CONTENTS
(Continued)

	<u>Page</u>
Definitions and Significance of Flexibility Factors	30
Determination of k_x and k_z	33
Other Load-Displacement Relationships	33
Flexibility Factors From CORTES-SA	34
Calculated Rotations	34
Beam Rotations	35
Flexibility Factors	35
Correlation Equations	36
Recommendations for k_x and k_z	40
5. CODE RECOMMENDATIONS	41
Limitations on Applicability	41
Recommendation for NB-3338.2(d)(3)	43
Recommendation for NB-3339.1(f)	43
Recommendation for NB-3686	44
Recommendations for Table NB-3681(a)-1	44
Recommendations for NB-3687.5 (Flexibility Factors)	46
6. REFERENCES	48
Figures 1 through 12 in numerical order	51-62
Tables 1 through 16 in numerical order	63-78

FOREWORD

The work reported here was performed at Oak Ridge National Laboratory and at Battelle-Columbus Laboratories under Union Carbide Corporation, Nuclear Division, Subcontract No. 2913 in support of the ORNL Design Criteria for Piping and Nozzles Program being conducted for the U.S. Nuclear Regulatory Commission, Office of Nuclear Regulatory Research. P. Albrecht of the Metallurgy and Materials Branch, Division of Reactor Safety Research, USNRC, is the cognizant RSR engineer and S. E. Moore of the Oak Ridge National Laboratory, Division of Engineering Technology, is the program manager.

The objectives of the ORNL program are to conduct integrated experimental and analytical stress analysis studies of piping system components and pressure vessel nozzles in order to confirm and/or improve the adequacy of structural design criteria and analytical methods used to assure the safe design of nuclear power plants. Activities under the program are coordinated with other safety related piping and pressure-vessel research through the Design Division, Pressure Vessel Research Committee (PVRC) of the Welding Research Council and through the ASME Boiler and Pressure Vessel Code Committees. Results from the ORNL program are used by appropriate Codes' and Standards' groups in drafting new or improved design rules and criteria.

The following reports have been issued under U.S. Nuclear Regulatory Commission sponsorship:

J. W. Bryson, J. P. Callahan, and R. C. Gwaltney, "Stress Analyses of Flat Plates with Attached Nozzles, Volume 1. Comparison of Stresses in a One-Nozzle-to-Flat-Plate Configuration and in a Two-Nozzle Configuration with Theoretical Predictions", ORNL-5044 (July, 1975).

R. L. Battiste et al., "Stress Analysis of Flat Plates with Attached Nozzles, Volume 2, "Experimental Stress Analyses of a Flat Plate with One Nozzle Attached", ORNL-5044 (July, 1975).

R. C. Gwaltney, J. W. Bryson, and S. E. Bolt, "Theoretical and Experimental Stress Analyses of ORNL Thin-Shell Cylinder-to-Cylinder Model 2", ORNL-5021 (October, 1975)

E. C. Rodabaugh and S. E. Moore, "Stress Indices for ANSI Standard B16.11 Socket-Welding Fittings", ORNL/TM-4929 (August, 1975).

- S. E. Moore, "Contributions of the ORNL Piping Program to Nuclear Piping Design Codes and Standards", Proceedings of the Technology Information Meeting on Methods for Analyzing Piping Integrity, November 11-12, 1975, ERDA-76-50; also in J. Press. Vessel Technol., Trans. ASME 99, 224-30 (February, 1977).
- W. L. Greenstreet, "Summary and Accomplishments of the ORNL Program for Nuclear Piping Design Criteria", Proceedings of the Technology Information Meeting on Methods for Analyzing Piping Integrity, November 11-12, 1975, ERDA 76-50.
- J. W. Bryson and W. F. Swinson, "Stress Analyses of Flat Plates with Attached Nozzles, Volume 3, Experimental Stress Analyses of a Flat Plate with Two Closely Spaced Nozzles of Equal Diameter Attached", ORNL-5044 (December, 1975)
- E. C. Rodabaugh, F. M. O'Hara, Jr., and S. E. Moore, "FLANGE: A Computer Program for the Analysis of Flanged Joints with Ring-Type Gaskets", ORNL-5035, (January, 1976).
- R. E. Textor, User's Guide for "SHFA: Steady-State Heat Flow Analysis of Tee Joints by the Finite Element Method", UCCND/CSD/INF-60, Oak Ridge Gaseous Diffusion Plant (January, 1976)
- E. C. Rodabaugh and S. E. Moore, "Flanged Joints with Contact Outside the Bolt Circle - ASME Part B Design Rules", ORNL/Sub/2913-1, Battelle-Columbus Laboratories (May, 1976).
- E. C. Rodabaugh, "Appropriate Nominal Stresses for Use With ASME Code Pressure-Loading Stress Indices for Nozzles", ORNL/Sub/2913-2, Battelle-Columbus Laboratories (June, 1976).
- S. E. Moore and J. W. Bryson, "Progress Report for the Design Criteria for Piping and Nozzles Program for the Two Quarterly Periods July 1 to September 30 and October 1 to December 31, 1975", ORNL/NUREG/TM-18 (June, 1976).
- R. L. Maxwell and R. W. Holland, "Experimental Stress Analysis of the Attachment Region of a Hemispherical Shell with a Radially Attached Nozzle, Zero Penetration", ORNL/Sub/2203-4, University of Tennessee (July, 1976).
- J. P. Callahan and J. W. Bryson, "Stress Analyses of Perforated Flat Plates Under In-Plane Loadings", ORNL/NUREG-2 (August, 1976)
- E. C. Rodabaugh and S. E. Moore, "Evaluation of the Bolting and Flanges of ANSI B16.5 Flanged Joints - ASME Part A Flanges", ORNL/Sub/2913-3, Battelle-Columbus Laboratories (September, 1976).
- E. C. Rodabaugh and R. C. Gwaltney, "Elastic Stresses at Reinforced Nozzles in Spherical Shells with Pressure and Moment Loading", ORNL/Sub/2913-4, Battelle-Columbus Laboratories (October, 1976).

- E. C. Rodabaugh, S. E. Moore, and J. N. Robinson, "Dimensional Control of Buttwelding Pipe Fittings for Nuclear Power Plant Class 1 Piping Systems", ORNL/Sub/2913-5, Battelle-Columbus Laboratories (December, 1976).
- S. E. Moore and J. W. Bryson, "Design Criteria for Piping and Nozzles Program Quarterly Progress Report for April-June 1976", ORNL/NUREG/TM-107 (April, 1977).
- E. C. Rodabaugh and S. E. Moore, "Flexibility Factors for Small ($d/D < 1/3$) Branch Connections with External Loadings", ORNL/Sub/2913-6, Battelle-Columbus Laboratories (March, 1977).
- S. E. Moore and J. W. Bryson, "Design Criteria for Piping and Nozzles Program Quarterly Progress Report for July-September 1976", ORNL/NUREG/TM-91 (February, 1977).
- P. G. Fowler and J. W. Bryson, "User's Manual for the CORTES Graphics Package GREPAK", ORNL/NUREG/TM-127 (August, 1977).
- B. R. Bass, J. W. Bryson, and S. E. Moore, "Validation of the Finite Element Stress Analysis Computer Program CORTES-SA for Analyzing Piping Tees and Pressure Vessel Nozzles". Pressure Vessels and Piping Computer Program Evaluation and Qualification, RVP-PB-024, pp. 9-25, ASME (1977).
- J. K. Hayes and S. E. Moore, "Experimental Stress Analysis for Four 24 in. ANSI Standard B16.9 Tees", Paper 77-PVP-4, presented at the ASME Energy Technology Conference and Exhibition, Houston, Texas, September 18-23, 1977.
- J. W. Bryson, W. G. Johnson, and B. R. Bass, "Stresses in Reinforced Nozzle-Cylinder Attachments Under Internal Pressure Loading Analyzed by the Finite-Element Method - A Parameter Study", ORNL/NUREG-4 (October, 1977).
- F. K. W. Tso et al., "Stress Analysis of Cylindrical Pressure Vessels with Closely Spaced Nozzles by the Finite-Element Method, Volume 1. Stress Analysis of Vessels with Two Closely Spaced Nozzles Under Internal Pressure", ORNL/NUREG-18/V1 (November, 1977).
- W. L. Greenstreet, "Experimental Study of Plastic Responses of Pipe Elbows", ORNL/NUREG-24 (February, 1978).
- E. C. Rodabaugh, S. K. Iskander, and S. E. Moore, "End Effects on Elbows Subjected to Moment Loadings", ORNL/Sub/2913-7, Battelle-Columbus Laboratories (March, 1978).
- E. C. Rodabaugh and S. E. Moore, "Evaluation of the Plastic Characteristics of Piping Products in Relation to ASME Code Criteria", NUREG/CR-0261, ORNL/Sub-2913/8, Battelle-Columbus Laboratories (July, 1978).
- F. K. W. Tso and R. A. Weed, "Stress Analysis of Cylindrical Pressure Vessels with Closely Spaced Nozzles by the Finite-Element Method, Volume 2, Vessels with Two Nozzles Under External Force and Moment Loadings", NUREG/CR-0132, ORNL/NUREG-18/V2 (August, 1978).

E. C. Rodabaugh and S. E. Moore, "Stress Indices for Girth Welded Joints, Including Radial Weld Shrinkage, Mismatch, and Tapered-Wall Transitions," NUREG/CR-0371, ORNL/Sub-2913/9, Battelle-Columbus Laboratories (September, 1978).

F. K. W. Tso and R. A. Weed, "Stress Analysis of Cylindrical Pressure Vessels with Closely-Spaced Nozzles by the Finite-Element Method, Vol. 3, Vessels with Three Nozzles Under Internal Pressure and External Loadings," NUREG/CR-0507, ORNL/NUREG-18/V3 (May, 1979).

ABSTRACT

Maximum stress intensities and flexibility factors for isolated nozzles in cylindrical portions of vessels and in straight pipe are evaluated. The major source of new data in this report was generated at Oak Ridge National Laboratory using the CORTES-SA computer program.

The new data, along with other available test and/or calculated data, are used to develop correlation equations for use in the Code. Recommendations for Code changes are included.

NOMENCLATURE

A = reinforcement cross sectional area

A_a = reinforcement area within Code boundaries

A_r = Code required minimum reinforcement area

C_1 = pressure loading primary-plus-secondary stress index

C_2 = moment loading primary-plus-secondary stress index

C_{2b} = moment on nozzle loading primary-plus-secondary stress index

C_{2r} = moment-through-vessel loading primary-plus-secondary stress index

D_i = inside diameter of vessel or run pipe

D_m = mean diameter of vessel or run pipe

D_o = outside diameter of vessel or run pipe

d_i = inside diameter of nozzle or branch pipe

d_o = outside diameter of branch pipe

d_m = mean diameter of nozzle, $= d_i + t_n$

E = modulus of elasticity

h = elbow parameter, defined under Equation (29)

I = moment of inertia

I_b = moment of inertia of branch pipe, $\cong \pi r^3 t$

K_1 = pressure loading peak stress index

K_2 = moment loading peak stress index

K_{2b} = moment on nozzle loading peak stress index

K_{2r} = moment-through-vessel loading peak stress index

k = flexibility factor

k_x = flexibility factor for rotation θ_{xn} due to M_{xn}

k_z = flexibility factor for rotation θ_{yn} due to M_{yn}

NOMENCLATURE
(Continued)

M_i = resultant moment

M_{ij} = moment applied to nozzle or vessel, see Figure 6.

P = internal pressure

R = mean radius of vessel or run pipe

r = mean radius of branch pipe

r_i = inside radius of nozzle, = $d_i/2$

r_p = outside nozzle radius, see Figure 2

r_1 = outside radius, see Figure 4

r_2 = inside radius, see Figure 4

T = wall thickness of vessel or run pipe

T_r = required minimum thickness of vessel or run pipe

t = wall thickness of branch pipe

t_n = wall thickness of nozzle, see Figure 4

X = tapered-reinforcement width, see Figure 4.

Y = dimension of P30-type reinforcement, see Figure 4.

Z = section modulus

Z_b = section modulus of branch pipe, using t and d_i

Z_v = section modulus of vessel, using T and D_i

θ = reinforcement angle, see Figure 4

θ_b = beam rotation (calculated nominal value)

θ_c = rotation obtained from CORTES-SA calculated displacement

θ_i = rotations used in deriving flexibility factors

NOMENCLATURE
(Continued)

$\bar{\sigma}$ = maximum calculated stress intensity for moment loading divided by M/Z_b for moment or nozzle or by M/Z_v for moment through vessel.

$\bar{\sigma}_c$ = maximum calculated stress intensity divided by $PD_m/2T$

$\bar{\sigma}_e$ = correlation Equation (18) stress intensity divided by $PD_m/2T$

$\bar{\sigma}_m$ = maximum measured stress intensity divided by $PD_m/2T$

1. INTRODUCTION

Nozzles in pressure vessels and piping pose a complex problem in stress analysis. To help alleviate the problem, stress indices for nozzles with pressure loading were introduced in the first (1963) edition of the Code*. Stress indices for nozzles with pressure, moment and thermal gradients were used in ANSI B31.7-1969 ^[1] and became part of the 1971 and later editions of the Code.

Stress indices for pressure loading are discussed in Chapter 2; stress indices for moment loading in Chapter 3. A stress index can be defined as a number which, when multiplied by an appropriate nominal stress, gives a significant stress. The concept is explained in an introductory section to each chapter, starting with the simplest example and working up to the complex aspects of stress indices for nozzle.

Flexibility factors are used in piping system analysis; that analysis gives (among other design information) the moments which act on nozzles. Flexibility factors are discussed in Chapter 4. A flexibility factor can be defined as a number which, when multiplied by an appropriate nominal rotation, gives a significant rotation. The concept is explained in the introductory section to Chapter 4, starting with the simplest example and working up to the complex aspects of flexibility factors for nozzles.

This report presents calculated and test data relevant to stress indices for pressure and moment loading and flexibility factors. The calculated data were obtained from Bryson, et al. ⁽³⁾ plus additional calculations performed by J. G. Johnson of UCCND Computer Sciences Division, Oak Ridge, Tennessee. As a consequence of the review of that data, several modifications of Code rules are suggested; these are summarized in Chapter 5.

* The term "Code" used herein refers to the ASME Boiler and Pressure Vessel Code, Section III - Division 1, 1977 Edition and Addendas as of December, 1978. Reference to portions of the Code are identified as in the Code; e.g., NB-3324.1.

2. STRESS INDICES FOR PRESSURE

Introduction

Stress Indices for Relatively Simple Geometries

A cylindrical shell (length of vessel or straight pipe) with closed ends is shown in Figure 1(a). If the shell is considered to be exactly circular in cross section with a constant thickness, T , then the stresses due to internal pressure at points remote from the closures are accurately given by the Lamé Equations:

$$S_h = \frac{P a^2 (b^2 + r^2)}{r^2 (b^2 - a^2)} \quad (1)$$

$$S_a = P \frac{a^2}{b^2 - a^2} \quad (2)$$

$$S_r = \frac{P a^2 (b^2 - r^2)}{r^2 (b^2 - a^2)} \quad (3)$$

where S_h = hoop-direction (tensile) stress
 S_a = axial-direction (tensile) stress
 S_r = radial-direction (compressive) stress
 a , b , and r are defined in Figure 1(a).

The maximum stress intensity occurs at the inside surface, $r = a$, and is given by:

$$S_{im} = S_h + S_r = P \frac{2b^2}{b^2 - a^2} \quad (4)$$

The average through-the-wall stress intensity is given by:

$$S_{ia} = \frac{1}{b-a} \int_a^b (S_h + S_r) dr = P \frac{2ba}{b^2 - a^2} \quad (5)$$

or, expressed in terms of mean diameter D_m and wall thickness T :

$$S_{ia} = \frac{PD_m}{2T} \left[1 - \left(\frac{T}{D_m} \right)^2 \right] \quad (6)$$

The Code, NB-3324.1, gives an equation for tentative thickness of cylindrical shells. This equation, solved for S in terms of D_m and T is:

$$S = \frac{PD_m}{2T} \quad (7)$$

Equation (7) for S is almost the same as Equation (6) for S_{ia} ; the average through-the-wall stress intensity. Indeed, even for shells with T/D_m as large as 0.1, the equations agree within one percent. We later use the nominal stress due to pressure defined by Equation (7); i.e.,

$$S_{nom} = PD_m / 2T \quad (8)$$

To illustrate the concept of stress indices, we can establish the magnitude of a stress index, I , for a cylindrical shell as the ratio of the maximum stress intensity to the nominal stress; Equation (4) divided by Equation (8):

$$I = \frac{S_{im}}{S_{nom}} = \frac{2b^2 P}{b^2 - a^2} \cdot \frac{2T}{PD_m} = 1 + \frac{T}{R_m} + \left(\frac{T}{2R_m} \right)^2 \quad (9)$$

For T/R_m of 0.2, $I = 1.21$; i.e. the maximum stress intensity in the cylindrical shell is $1.21 \times (PD_m/2T)$. For $T/R_m = 0.02$, $I = 1.0201$. These indices would be exact if, in fact, the length of vessel or pipe were an idealized cylindrical shell with uniform wall and exactly circularly cross section. A slightly out-of-round cross section may increase stresses significantly; this is explicitly recognized in NB-3600 and stress indices are provided for out-of-round pipe.

The more complex geometry of a curved pipe is shown in Figure 1(b). The hoop stresses now vary as a function of the coordinate angle, ϕ . An exact theory for thick-wall curved pipe is not available. Shell theory indicates that the axial stress is the same as in straight pipe but that the hoop stress is given by:

$$S_h = \frac{PD}{2T} \frac{2R + r \sin\phi}{2(R + r \sin\phi)} \quad (10)$$

where: R = bend radius, r = cross section radius.

Equation (10) indicates that S_h is a maximum at $\phi = -90^\circ$. Accordingly, I for an elbow can be expressed as

$$I = \frac{2R - r}{2(R - r)} \quad (11)$$

To insure conservatism for thick-wall elbows, NB-3600 uses the above stress index with a nominal stress of $PD_o/2T$. The index is accurate for thin-wall curved pipe at locations remote from attached pipe or other end-attachments provided the cross-section is round. NB-3600 provides stress indices for out-of-round elbows.

Stress Indices for Nozzles

The more complex geometries of nozzles in vessels or piping are shown in Figure 2. Stress indices for nozzles in cylindrical shells are shown in Table 1. These indices have not been changed since their introduction in the first (1963) edition of the Code. They are presumably based on photoelastic test data available at that time.

NB-3338.2 states that:

"The term stress index, as used herein, is defined as the numerical ratio of the stress components, σ_t , σ_n , and σ_r under consideration to the computed membrane stress in the unpenetrated vessel material; however, the material which increases the thickness of a vessel wall locally at

the nozzle shall not be included in the calculations of these stress components."

Now, this is a rather wordy definition but nevertheless quite vague. How does one compute the membrane stress in the unpenetrated vessel material? Does one use Equations (1), (2), (4), (5) or (7) herein? All five equations seem like potential candidates.

NB-3339.7 (NB-3339 is Alternative Rules for Nozzle Design) states that:

"The term stress index, as used herein, is defined as the numerical ratio of the stress components, σ_t , σ_n and σ_r under consideration to the computed stress, S".

S is defined by the equation (in our terminology)

$$S = PD_m/2T \quad (12)$$

Equation (12) is identical to Equation (7). If we look at the test data available in 1963 (NB-3338.1 states that the indices are based on test data) we find that the stress indices were developed using the nominal stress defined by Equation (12). Presumably, the intent of the wordy definition in NB-3338.2 is the same as that in NB-3339.7.

However, if in fact the intent of NB-3338.2 is the same as NB-3339.7, then there is an error in Table NB-3338.2(c)-1 (Table 1 herein) in defining the stress index for σ_r on the inside surface as $(-t_n/R)$. The symbol t_n is defined as the nozzle wall thickness, see Figure 2 herein. Now σ_r on the inside surface can only be $-P$ and, with the nominal stress defined as $PD_m/2T$, the stress index must be $-2T/D_m$. Table NB-3339.7-1 shows the index correctly; otherwise the tables of stress indices for the alternative rules of NB-3339 are identical to those in Table 1 herein.

Some history of stress indices for pressure since the 1974 edition of the Code is pertinent at this point because that history has considerable bearing on our objective in the remainder of this chapter. In 1974, NB-3338.2 stated:

"The term stress index, as used herein, is defined as the numerical ratio of the stress components, σ_t , σ_n , and σ_r under consideration to the computed membrane stress in the unpenetrated and unreinforced vessel material."

This definition is vague, like the present description. Did it, for example, permit one to obtain stresses at openings by multiplying the stress index by the axial membrane stress? Perhaps, but users of this portion of the Code apparently multiplied the stress index by something like $PD_m/2T$ to obtain stresses.

In 1974, NB-3339.7 read like at present with one significant exception: S was defined as:

$$S = PD_m/2T_r$$

when T_r was the required minimum thickness of the vessel as computed by the equation $T_r = PR_i/(S_m - 0.5P)$. This constituted a clear definition of the multiplier of the stress indices to obtain stresses.

The significance of using T or T_r in defining the nominal stress can be discussed in terms of Figure 2(d). Let us assume that t_n is exactly that required for supporting the pressure as a cylindrical shell; in which case there is no available reinforcing area in the nozzle. Let us also assume that the diameter of the opening is such that the area under radius r_2 is insignificant compared to the required reinforcement area, $d_i T_r$. The question arises; can this type of nozzle meet the Code reinforcing rules? If it does not, the stress indices can not be used. The answer, of course, is: Yes. For given d_i and T and no available reinforcement in the nozzle, there is always some T_r for which the Code reinforcement rules are satisfied. Indeed, for a fairly broad range of parameters, the Code reinforcement rules are satisfied if $T/T_r \geq 2.0$.

Now, we ask the question, "For a nozzle like Figure 2(d) with no significant reinforcing in the nozzle, can the stress indices in Table 1 when used with the nominal stress $PD_m/2T$ be defended as being accurate, or if not accurate, at least conservative?" The answer is: No. Reference [2], in discussing the subject, cited published tests and theories which showed

that stresses could be two or three times as high as stresses calculated from the stress indices of Table 1 used with a nominal stress of $PD_m/2T$.

Now suppose we use a nominal stress of $PD_m/2T_r$ in conjunction with the stress indices of Table 1. It turns out that with this nominal stress the indices* can be defended as conservative. However, a conceptual difficulty arises with this definition of nominal stress, as illustrated in Figure 3. We start with Figure 3(a). For the sake of an explicit example, we assume we are in the rather broad range of parameters for which making $T = 2T_r$ satisfies Code reinforcement requirements.

In Figure 3(a), the thickness T could be fabricated by adding a pad of weld metal or by installing a complete or partial shell course of thicker plate. Reinforcement of the opening is accomplished by the added shaded area in Figure 3. We do not have much data on this type of configuration but such data as are available indicates that, in particular, the stress at the inside corner (longitudinal plane, inside) would not exceed $3.3 (PD_m/2T_r)$. Presumably, the intent of the present wording of NB-3338.2, "however, the material which increases the thickness of a vessel wall locally at the nozzle shall not be included in the calculation of these stress components" is intended to suggest to the user that if he has a configuration like Figure 3(a), he should use $PD_m/2T_r$ as the nominal stress; not $PD_m/2T$.

Figure 3(b) is just like Figure 3(a) except now the thickened shell course is longer. We do not have test data on what effect this would have on the stresses at, in particular, the inside corner. However, we would judge that it would not be much. For example, if for Figure 3(a) the stress at the inside corner were $2.5 (PD_m/2T_r)$, for Figure 3(b) the stress at the inside corner might be $2.3 (PD_m/2T_r)$. However, the definition under NB-3338.2 might be interpreted as "use a nominal stress of $(PD_m/2T)$. The calculated stress for Figure 3(b) would then be one-half of that for Figure 3(a). The magic change under NB-3338.2 occurs when "thickness of the vessel locally" changes to thickness of the vessel not locally. What is meant by "locally" is not defined. If a nominal stress of $PD/2T$ is used, it can be readily shown that the stress will be grossly underpredicted for certain

* Except, of course, the erroneous index of $-t_n/R$ in Table NB-3338.2(c)-1.

parameters within the range of coverage in the 1974 edition of the Code. If one uses a nominal stress of $PD_m/2T_r$ for Figure 3(b), the calculated stresses will be exactly the same as for Figure 3(a). If, in fact, lengthening the shell course does lower the stresses at the inside corner then the stress indices/nominal stress of $PD_m/2T_r$ will be more conservative for Figure 3(b), than for Figure 3(a), but conservative for both.

Figure 3(c) illustrates the conceptual difficulty with the use of the nominal stress $PD_m/2T_r$. The shell course is very long and T is $4T_r$. This is a heavily over-reinforced nozzle in terms of Code reinforcement requirements. Using a nominal stress of $PD/2T_r$ means that the calculated stress (for a given pressure) for Figure 3(c) is exactly the same as for Figure 3(a). Is this an accurate description of the relative magnitude of the stresses at the inside corner? The answer is: No. If, for example, the stress at the inside corner of Figure 3(a) is $2.5 (PD_m/2T_r)$, the stress at the inside corner of Figure 3(c) would be about $(1/2) \times 2.5 (PD_m/2T_r)$.

Before proceeding with the historical solution to the dilemma described above, it is pertinent to discuss a related aspect of importance throughout the report. The reader, in looking at Figure 3(c), may have asked himself a pertinent question: Where, in Class 1 vessels or piping in light water cooled reactors will there ever be a configuration like Figure 3(c)? Insofar as we are aware, the answer is: Nowhere. However, it should be noted that the stress indices of Table 1 are stated to be applicable for D_i/T up to 100 and, for LMFBR piping in particular, a configuration like Figure 3(c) could be encountered. Indeed, the inquiry which prompted the review discussed in Reference [2], and which prompted certain Code changes discussed later, came from an LMFBR piping application. To the extent that the Code indices are being used for high temperature design, the need exists to examine the validity of the indices and nominal stresses for D_i/T up to 100 and configurations like Figure 3(c). Further, Class 1 stress indices are useable, to some extent, for Class 2 and 3 piping and here again D_i/T up to 100 and configuration like Figure 3(c) might be encountered.

Returning now to the dilemma: Using a nominal stress of $PD_m/2T$ can be shown to be unconservative for certain parameters; using a nominal stress of $PD_m/2T_r$ can be shown to be illogical and excessively conservative for configurations like Figure 3(c). Reference [2], based on data available at

that time, suggested that for the parameter $(d_i/D_i) \sqrt{D_i/T} < 0.6$, the stress index of 3.1 for the inside corner used with a nominal stress of $PD_m/2T$ would not be unconservative. Pressure vessel designers reviewed nozzles used in PWR's and BWR's and found that most nozzles had d_i/D_i and D_i/T such that $(d_i/D_i) \sqrt{D_i/T} < 0.6$. However, there were some slightly above the limit and they noted that Reference [2] stated that the limit could be stretched up to 0.7 or 0.8 with no great amount of unconservatism. Accordingly, a limit of $(d_i/D_i) \sqrt{D_i/T} = 0.8$ was selected and made part of the Code in NB-3338.2(d)(3) and NB-3339.1.

While this solved the dilemma for the NB-3300 (pressure vessel) portion of the Code, the dilemma remained for the NB-3600 (piping) portion of the Code. In piping, $(d_i/D_i) \sqrt{D_i/T} > 0.8$ is frequently encountered; particularly with the needs of LMFBR piping in mind.

In NB-3600, the analog of the index for $S = 3.3$ for the inside corner appears as a C_1K_1 - index for "Branch Connections per NB-3643". It is used in the Code equation for calculating peak stress intensity, S_p :

$$S_p = C_1K_1 \frac{PD_o}{2T} + \dots \text{ other terms for other loads} \quad (13)$$

where T is the run pipe wall thickness; not the minimum required thickness, T_r . At present, $C_1 = 2.0$, $K_1 = 1.7$, $C_1K_1 = 3.4$. The indices are in the process of being changed to $C_1 = 1.5$, $K_1 = 2.2$; that aspect is discussed at the end of this chapter. For the present, we note that for $C_1K_1 = 3.4$ or 3.3 , and even with the slightly more conservative nominal stress using D_o rather than D_m , the term $C_1K_1 PD_o/2T$ will be unconservative for large values of d_i/D_i combined with large values of D_i/T in a configuration like 3(c). For example, the parametric study discussed subsequently herein includes a Model U2TA with $D_i/T = 50$, $d_i/D_i = 0.5$; the calculated inside corner stress intensity is 8.22 ($PD_m/2T$) or 8.06 ($PD_o/2T$). This is 2.4 times the stress given by $S_p = 3.4 (PD_o/2T)$.

The NB-3600 (Piping) portion of the Code includes a Table NB-3686.1-1 which contains a set of stress indices like Table 1 herein, but with σ_r on the inside surface correctly defined, and with a conservative

nominal stress of $PD_m/2T_r^*$. Accordingly, these indices/nominal stress can be defended as conservative but can be criticized as excessively conservative for configurations like Figure 3(c). However, Table NB-3686.1-1 apparently is seldom if ever used, hence we have little motivation to modify it and, indeed, recommend that it (and associated text) be deleted from the Code. In the following, therefore, we confine our attention to the maximum stress intensity due to internal pressure; the equivalent of the C_1K_1 - index in Equation (13) and S for the inside corner in Table 1.

This study does not cover all possible configurations of nozzles. Rather, it is concerned with the four specific configurations illustrated by Figure 2(a), (b), (c), and (d)

Calculated Stresses

Bryson, et al. [3] give results of a parametric study of nozzles in vessels using the computer program CORTES-SA. The parametric study included three configurations:

- U-models, Figure 4(a)
- S-models, Figure 4(b)
- P30-models, Figure 4(c)

Dimensional ratios for the 25 models are shown in Table 2. The ratios D_i/T and d_i/D_i were selected for the study. The pipe wall thickness was established by $t = (d_i/D_i)T$. The radii r_1 and r_2 were established as $r_1 = T/2$ and $r_2 =$ larger of $t_n/2$ or $T/2$. Dimensions t_n and L_n were established for the SI-models by the equations:

$$A = d_i T = 2L_n (t_n - t) \quad (14)$$

$$2L_n = [0.5 (d_i + t_n) t_n]^{1/2} + r_2 \quad (15)$$

* The Code contains a typo error in NB-3686.3(a). The quantity PR_r/t_m should be PR_m/t_r . R_m is defined as mean radius of run pipe, t_r is defined as minimum required thickness of run pipe, calculated as a plain cylinder. Neither R_r or t_m are defined.

Equations (14) and (15) were solved simultaneously for the values of t_n and L_n .

Equation (14) represents the required area of reinforcement of NB-3333.2. Equation (15) represents the limit of reinforcement normal to the vessel wall of NB-3334.2. The limit of reinforcement along the vessel wall is also met by S1-models. Accordingly, the S1-models just meet the Code reinforcement requirements for nozzles in vessels where the required vessel wall is equal to T and the required minimum pipe wall is $t = (d_i/D_i)T$. The S1-models, except for S1A, S1B and S1C, also meet the reinforcement requirements of NB-3339; the Code alternative rules for nozzle design.

For the P30-models, Figure 4(c), the X-dimension was selected so that the area of reinforcement, $1.732X^2$, was equal to the NB-3332.2 required area of reinforcement, $d_i T$. However, the P30-models do not meet NB-3331 and NB-3334 rules for required vessel wall equal to T because Y is greater than L_n , where, by NB-3334.2 definition:

$$L_n = 0.5 [(r_i + 0.5 t_n)t_n]^{1/2}$$

$$t_n = t + (2/3) X$$

Ratios of L_n/Y and A_a/A_r (available area/required area) are:

Model	L_n/Y	A_a/A_r
P30 A	0.503	0.753
B	0.424	0.668
C	0.380	0.616
D	0.350	0.577
E	0.253	0.442

Accordingly, while the P30-models have compact and well-proportional reinforcement, and the total reinforcement area is the required $d_i T$, they do not meet the NB-3331 and NB-3334 rules. P30-models (except P30 A), however, do meet the NB-3339 rules for required vessel wall = T . This is because the

NB-3339 rules for these particular models require less reinforcing area and provide a larger reinforced zone boundary than NB-3331 and NB-3334 rules.

In order to obtain a more complete basis for establishing correlation equations, calculations of stresses due to pressure were also made for the additional models shown in Table 3. The dimensions of these models were derived from Table 2 models as follows.

U2T-Models

The vessel wall thickness of U2T-models is twice that of the corresponding UT-models. Dimensions D_i , d_i , t , r_1 and r_2 were not changed.

S75, S50 and S25-Models

The nozzle wall thickness, t_n , was established by the equation:

$$t_n = (t'_n - t) k + t \quad (16)$$

where t'_n is the nozzle wall thickness for the S1-models, t = pipe wall thickness [= $(d_i/D_i)T$, as in S1-models] and $k = 0.75, 0.50$ and 0.25 for S75, S50 and S25-models, respectively.

Calculated values of the normalized (divided by $PD_m/2T$) maximum stress intensity are shown in Tables 2 and 3 under the heading $\bar{\sigma}_c$. The maximum stress intensities were located at or near the inside corner; for most models the stress intensity consists of a high tensile stress normal to the transverse plane plus the internal pressure.

Test Data

To supplement the calculated stress data and provide additional guidance for developing a correlation equation, published data giving results of tests on photoelastic models with internal pressure loading were compiled; these data are summarized in Table 4. Other photoelastic test data on nozzles in cylindrical shells with pressure loading are available in Refer-

Reference [4] and [23]; however they are not compatible with the present study either because $d_m/D_m > 0.5$ or the configuration is not included in Figure 2.

The maximum stress intensity always occurred at the "inside corner" and consisted of a stress normal to the longitudinal plane plus the compressive stress due to pressure*. All of these models had inside corner radii (r_1) varying from about $0.1T$ to T . Inside corner radii within this range have relatively little effect on maximum stress intensity.

Additional photoelastic test data from Seika, et al. [8] are shown in Table 5. Maximum stresses were found to be at the inside corner in the longitudinal plane and normal to that plane. We have added the pressure to the reported maximum stresses to obtain the stress intensities shown in the column headed $\bar{\sigma}_m$ in Table 5. Reference [8] gives results only in the form of small graphs which are readable only to about ± 0.1 ; hence the round-off of the values of $\bar{\sigma}_m$. These models had square inside corners ($r_1 = 0$) which poses problems in the photoelastic analysis. The authors of Reference [8] state that "the actual stress obtained from the slice 2 mm in thickness at the corner was regarded as the maximum stress in this investigation". (The wall thickness of the cylindrical shell was ~ 7.0 mm.)

Test data from steel models using strain gages are summarized in Table 6. These test data will be discussed further in the following section of "Correlation Equations".

Correlation Equations

Having obtained calculated and measured data on maximum stress intensities for nozzles in vessels, a correlation equation was sought to use in obtaining $\bar{\sigma}_e$ for nozzles with intermediate or (within reason) extrapolated values of the dimensions: D_m , T , d_m , t_n and r_2 . Because there are five independent dimensions, the correlation equation can be expressed as a function of four ratios of dimensions. We elected to use the functional form:

* One exception: Model E1 where the maximum stress intensity consists of the stress at the inside corner normal to the longitudinal plane plus a negative tangential stress at the inside corner.

$$\bar{\sigma}_e = a_1 \left(\frac{D_m}{T}\right)^{a_2} \left(\frac{d_m}{D_m}\right)^{a_3} \left(\frac{t_n}{T}\right)^{a_4} \left(\frac{r_2}{t_n}\right)^{a_5} \quad (17)$$

By using the logs of the ratios, a multiple linear regression analysis was performed using the data given in Tables 2, 3, and 4. This establishes the constants a_2 , a_3 , a_4 , and a_5 . The constant a_1 can be chosen so the $\bar{\sigma}_e$ represents an average of the data; or any other selected relationship between $\bar{\sigma}_e$ and the test data. We elected to choose a_1 so that $\bar{\sigma}_e$ essentially represents an average of the data in Tables 2 and 3. The resulting equation is:

$$\bar{\sigma}_e = 2.8 \left(\frac{D_m}{T}\right)^{.1815} \left(\frac{d_m}{D_m}\right)^{.367} \left(\frac{t_n}{T}\right)^{-.382} \left(\frac{r_2}{t_n}\right)^{-.148} \quad (18)$$

This equation gives a mean error \bar{x} of +1.94% and variance, s , of 10.8% with respect to the CORTES data (Tables 2 and 3); and $\bar{x} = +19.25\%$, $s = 11.8\%$ with respect to the photoelastic data of Table 4. Further justification for the choice of $a_1 = 2.8$ is based on fatigue strength considerations as discussed later in this Chapter.

Comparison With Test Data

Photoelastic Test Data

Equation (18) is plotted in Figure 5. The calculated data tend to be above Equation (18) for thick walled vessels ($D/T = 10$) and slightly below Equation (18) for thin-walled vessels ($D/T > 40$), while the photoelastic data tend to lie below (18). Indeed, on the average the photoelastic data is about 17% lower than the calculated data. There has been speculation on the significance of photoelastic tests, where the material has a Poisson's ratio of about 0.5, to actual (steel) nozzles, where the material has a Poisson's ratio of about 0.3. Mershon ^[14] cites calculated stresses of nozzles in spherical shells, using Poisson's ratio values of 0.3 and 0.5, which suggest that the inside corner stress would be less for Poisson's ratio of 0.5 than for Poisson's ratio of 0.3.

Comparison of Equation (18) with photoelastic test data from Seika, et al. [8] are shown in the last two columns of Table 5. The average of $\bar{\sigma}_e/\bar{\sigma}_m$ is 1.187 and, because Equation (18) is about 2% above the average of the calculated data, this set of photoelastic data is also about 17% lower than the calculated data.

Steel Models Test Data

Comparison of Equation (18) with test data from steel models is shown in the last two columns of Table 6. While we do not have Poisson's ratio to consider in these comparisons; strain gage tests are subject to the problem of making sure that a small strain gage is placed at the location of maximum stress intensity.

From a geometry standpoint, Reference [9] and [12] tests are most suitable for comparison with Equation (18). These models had defined fillet radii (r_2) and ratios D_m/T , d_m/D_m , t_n/T and r_2/t_n within the range of the parameter study. Reference [12] Model R was well instrumented with small strain gages in the critical region. Reference [9] indicates nothing about size of gages but there was at least one gage near the inside corner. In these four tests, the average of $\bar{\sigma}_e/\bar{\sigma}_m$ is 1.118 and, because Equation (18) is about 2% below the average of the calculated data, these four data on steel models are about 10% lower than the calculated data. The four P30-type models (Reference [10], Model 6, and Reference [11]) $\bar{\sigma}_e/\bar{\sigma}_m$ average is 1.064; we do not include Reference [10] Model 9 in this group because r_2/t_n is below the range of applicability of Equation (18).

For Reference [10] Models 2, 8, and 11, there was a fillet weld rather than a radius and we arbitrarily set r_2 equal to the fillet weld leg. The average of $\bar{\sigma}_e/\bar{\sigma}_m$ for all the models in Table 6 is 1.096.

Reference [13] models were intentionally made with r_1 and r_2 as close to zero as possible. For purposes of computer program validation however, the authors of Reference [3] used a value of $r_2 = 0.01$ for Models 1 and 3; we have used the same value in calculating $\bar{\sigma}_e$. The values $\bar{\sigma}_m$ given in Table 6 are estimates of the maximum stress intensities obtained by averaging the extrapolated gage readings given in Reference [13] along the nozzle and cylinder sides of the intersection. For Model 1, $\bar{\sigma}_m$ occurs on the outside surface at the intersection. For Models 3 and 4, $\bar{\sigma}_m$ occurs at the inside corner.

In summary, the available test data on steel models is insufficient to establish a firm judgement on the validity of the calculated data. However, the available data suggests that the calculated data may be slightly on the high side and that Equation (18), based on the average of the calculated data, is generally conservative.

Comparison With Reference [15] Finite-Element Analysis

Truitt & Raju [15] give results of a finite element analysis of a nozzle in a vessel with dimensional ratios within the range of our parametric study, using an analysis technique comparable to CORTES-SA. The configuration is slightly different than our S-type models in that the bore is tapered by 5.4°. Using an average bore diameter, the dimensional ratios are:

$$\frac{D_m}{T} = 18.3 \quad , \quad \frac{d_m}{D_m} = 0.261 \quad , \quad \frac{t_n}{T} = 1.340 \quad , \quad \frac{r_2}{t_n} = 0.497$$

Equation (18) gives $\bar{\sigma}_e = 2.88$. Reference [15] gives the normalized maximum principle stress as 2.62; this occurs at the inside corner. Adding to this the radial stress due to internal pressure, $2/(D_m/T)$, gives the normalized maximum stress of $2.62 + 0.11 = 2.73$ as compared to 2.88 by Equation (18). Recalling that the average of CORTES-SA data is about 2% lower than Equation (18), Reference [15] $\bar{\sigma}_c$ is about 8% lower than CORTES-SA, and about 6% lower than Equation (18).

Influence of L_n in S-Type Models

It can be seen in Figure 4(b) that in S-type models the nozzle thickness extends only through the length $L_n = \{[0.5 (d_i/t_n) t_n]^{1/2} + r_2\}/2$. However in the test models (other than P30-type), the thickness t_n extends much further. In comparing the CORTES-SA data with the test models we are making an implicit assumption that the added nozzle thickness beyond L_n does not affect the stress at the inside corner. We do not have any direct evidence that this assumption is valid and, indeed, the general tendency for test data to be lower than CORTES-SA calculated data may be partially or entirely due to the influence of the material beyond L_n in the test models.

Stress Indices for Nozzles Meeting Code Rules

Having established correlation Equation (18), we use it in the following to calculate stress indices for nozzle which represent bounds of those permissible under Code rules; both NB-3331/NB-3334 rules and NB-3339 rules.

Sl-Type Nozzle

Table 7 shows stress indices calculated by Equation (18) for nozzles which just meet NB-3331/NB-3334 rules. Two steps are involved. First, for selected values of D_i/T and d_i/D_i and with $t = (d_i/D_i)T$, $r_2 =$ larger of $0.5T$ or $0.5t_n$, we use Equations (14) and (15) to calculate t_n/T . Having all of the parameters involved in Equation (18), we use it to calculate the stress index, $\bar{\sigma}_e$.

An exception to the use of Equations (14) and (15) occurs where $(d_i/D_i) \sqrt{D_i/T}$ is less than 0.1414. NB-3332.1 states that no reinforcement is required for such nozzles and hence as a bound, $t_n/T = t/T = (d_i/D_i)T$.

Table 8 shows stress indices calculated by Equation (18) for nozzles which just meet NB-3339 rules. Two steps are involved. First, for selected values of D_i/T and d_i/D_i and with $t = (d_i/D_i)T$, we obtain the required minimum value of t_n/T using the reinforcement rules of NB-3339. These rules can be expressed by the equation:

$$2 \times 0.75 (T/D_i)^{2/3} D_i (t_n - t) = a d_i T \quad (19)$$

where $a = 0$ for $\rho < 0.1414$; $\rho = (d_i/D_i) \sqrt{D_i/T}$

$$a = 4.816 \rho^{1/2} - 1.81 \text{ for } 0.1414 < \rho < 0.2828$$

$$a = 0.75 \text{ for } \rho > 0.2828$$

Equation (19) may be written as:

$$\frac{t_n}{T} = \left[\frac{a}{1.5} \left(\frac{D_i}{T} \right)^{2/3} + 1 \right] \frac{d_i}{D_i} \quad (20)$$

Having all the parameters in Equation (18), we use it to calculate the stress index, $\bar{\sigma}_e$.

It can be seen in Tables 7 and 8 that maximum stress intensity indices are (with the exception of $D_i/T = 40$, $d_i/D_i = 0.02$) all below the stress index of $S = 3.3$ in Table 1 or below $C_1 K_1 = 3.3$. The alternative rules of NB-3339 provide a more uniform design in that $\bar{\sigma}_e$ (except for asterisked entries) ranges from 2.71 to 3.33 as compared to 1.93 to 3.25 for the "standard rules". The average index is a bit higher for the alternative rules as compared to the "standard" rules, as might be expected from the lower required reinforcement area under the alternative rules.

U2T-Type Nozzles

Table 9 shows stress indices calculated by Equation (18) for nozzles which meet NB-3331/NB-3334 and NB-3339 rules by excess thickness in the vessel or run pipe. For this bound, t_n/T is equal to t/T and d_i/D_i . It may be observed that Table 9 is a complete set of the entries astericked in Tables 7 and 8.

Table 9 provides an assessment of the adequacy of the present Code limit on applicability of the stress indices in NB-3300 to $(d_i/D_i) \sqrt{D_i/T} < 0.8$. The heavy line through Table 9 divides the nozzles into those with $(d_i/D_i) \sqrt{D_i/T} < 0.8$; those above or to the left on the line, and nozzles with $(d_i/D_i) \sqrt{D_i/T} > 0.8$; those below or to the right of the line. It can be seen that the Code limit does not assure that maximum stress intensities will be less than 3.3 ($PD_m/2T$).

One could suggest decreasing the Code limit to $(d_i/D_i) \sqrt{D_i/T} < 0.6$, as originally proposed in Reference [2]. However, it can be seen from Equation (18) that $\bar{\sigma}_e$ is not a function of $(d_i/D_i) \sqrt{D_i/T}$ alone. We can write Equation (18) in the special form for all reinforcing in the vessel or run pipe as:

$$\begin{aligned}\bar{\sigma}_e &= 2.8 \left(\frac{D_i}{T} + 1 \right)^{.1815} \left(\frac{d_i}{D_i} \right)^{.367} \left(\frac{d_i}{D_i} \right)^{-.382} \left(\frac{0.5}{d_i/D_i} \right)^{-.148} \\ \bar{\sigma}_e &= 3.102 \left(\frac{D_i}{T} + 1 \right)^{.1815} \left(\frac{d_i}{D_i} \right)^{.133}\end{aligned}\tag{21}$$

To assure that the maximum stress does not exceed 3.3 ($PD_m/2T$), we can impose the limitation on use of the stress indices as

$$\left(\frac{D_i}{T} + 1 \right)^{.1815} \left(\frac{d_i}{D_i} \right)^{.133} < \frac{3.3}{3.102}\tag{22}$$

For simplicity, we would like to use D_i/T rather than $(D_i/T + 1)$. Values of $D_i/T < 10$ are seldom encountered, hence we can reasonably replace $(D_i/T + 1)$ with $(D_i/T) \times 11/10$. This leads to the limit

$$\left(\frac{D_i}{T} \right)^{.1815} \left(\frac{d_i}{D_i} \right)^{.133} < \frac{3.3}{3.102 \times (11/10)^{.1815}} = 1.045\tag{23}$$

We recommend that the limit $(d_i/D_i) \sqrt{D_i/T}$ (d/\sqrt{Dt} in Code terminology) < 0.8 in NB-3338.2(d)(3) and NB-3339.1(f) be replaced by

$$\left(\frac{d_i}{D_i} \right)^{.133} (D_i/T)^{.18} < 1.1\tag{24}$$

Recommendations for C_1 and K_1

An appropriate value for the $K_1 C_1$ -product, for "Branch connections per NB-3643" is deemed to be Equation (18) herein. The question arises: What fraction of $C_1 K_1$ should be assigned to C_1 ? The C_1 -index is intended to represent the primary-plus-secondary stress intensity, S_n . The $K_1 C_1$ -product is intended to represent the primary-plus-secondary-plus peak stress intensity, S_p . The distinction becomes significant if S_n (from pressure and other loads) exceeds $3S_m$.

The aspect of dividing $C_1 K_1$ into appropriate fractions is discussed at some length in Reference [28] for piping products in general, and specifically for nozzles and branch connections in Reference [16]. Although neither the Code [2] nor the Code Criteria [29] give specific attention to this question, it is clear that the "intent" of the Code procedures is to ensure both shakedown to elastic behavior under cyclic loading and an adequate safety margin against fatigue failure. The design fatigue curves of the Code (Figures I-9.0 - I-9.4) include safety factors of 2 on strain-range or 20 on cycles-to-failure, whichever is greater, with respect to the average data base. An appropriate criterion for dividing $C_1 K_1$ is thus to assure that the resulting indices used in conjunction with the design procedures provide at least an average cycles-to-failure safety-factor of 20 for the available experimental data, as proposed in Reference [16]. Following this approach the recommendations for C_1 and K_1 are that, in Table NB-3681(a)-1, opposite "Branch Connections per NB-3643" replace the present values of C_1 and K_1 with an appropriately numbered footnote as follows:

$$C_1 = 1.4 \left(\frac{D}{T} \right)^{0.182} \left(\frac{d}{D} \right)^{0.367} \left(\frac{t}{T} \right)^{-0.382} \left(\frac{r_2}{t} \right)^{-0.148} \quad (25)$$

but not less than 1.2.

$$K_1 = 2.0. \quad (26)$$

Using Equations (25) and (26) and the analysis procedures of NB-3650 to interpret the fatigue data in Reference [16] gave safety factors ranging from 3.7 to 62.8 for Pickett and Grigory [30] and from 7.3 to 278 for Kameoka et al. [31] with average values of 25.8 and 54.5, respectively.

The limitations associated with the Code use of stress indices for nozzles in vessels or piping are discussed in Chapter 5, along with a summary of recommended Code changes.

STRESS INDICES FOR MOMENTS

Introduction

Stress Indices for Relatively Simple Geometries

A length of straight pipe subjected to moment loads is shown in Figure 6(a). The magnitudes of the moments are obtained from an analysis of the piping system. In general, the moments vary along the pipe axis but, at any specific location, a specific set of moments will be known. Moments M_1 and M_2 are not distinguished with respect to the pipe geometry; they can be combined to a single moment, $M_b = (M_1^2 + M_2^2)^{1/2}$. The bending moment M_b gives axial stresses which vary around the pipe; the maximum stresses are equal to $\pm M_b/Z$. The shear stress, S_s , due to the torsional moment is $M_3/2Z$. The maximum stress intensity, S_i , is then:

$$S_i = \left[S_a^2 + (S_s)^2 \right]^{1/2} \tag{27}$$

$$= \frac{(M_1^2 + M_2^2 + M_3^2)^{1/2}}{Z}$$

The Code procedure entails the calculation of the "Peak Stress Intensity Range" for moment loading ranges by the term:

$$S_p = K_2 C_2 \frac{M_i}{Z} \tag{28}$$

where, for straight pipe, $C_2 = K_2 = 1.0$ and $M_i = (M_1^2 + M_2^2 + M_3^2)^{1/2}$. Accordingly, for straight pipe, the Code procedure leads to an "exact" representation of the maximum stress intensity due to moment loads; i.e., Equation (27) is identical to Equation (28).

The more complex geometry of a curved pipe is shown in Figure 6(b). The moments M_1 and M_2 are distinguished with respect to the curved pipe geometry and, in general, the maximum stress intensity is not equal to M_1/Z . Indeed, the maximum stress intensity due to M_2 is given by:

$$S_m = \frac{1.95}{h^{2/3}} \frac{M_2}{Z} \quad (29)$$

where $h = tR/r^2$ [Equation (29) is valid for $h < \sim 1.0$]
 t = wall thickness
 R = bend radius
 r = cross section radius

For some curved pipe, the factor $1.95/h^{2/3}$ can be significantly greater than unity. For example, the h for a 24" ANSI B16.9 elbows ($R = 36"$) with 0.50" wall thickness is 0.130 and $1.95/h^{2/3} = 7.60$. Accordingly, this with Equation (29) means that the maximum stress intensity is 7.6 times the maximum stress intensity in a straight pipe with the same r and t , subjected to the same bending moment. The maximum stress intensity in the elbow is in the hoop-direction (not axial) at the sides of the elbow and is a through-the-wall bending stress.

The moment M_2 applied to curved pipe is often called an in-plane moment. The moment M_1 , called an out-of-plane moment, gives maximum stress intensities that are about 86% of those for M_2 (both for small values of h). The maximum stress intensities are also bending stresses in the hoop direction but located about 45° away from those produced by M_2 . The torsional moment M_3 produces shear stresses just like in straight pipe; i.e. $S_s = M_3/2Z$.

For curved pipe, an upper bound on the stress intensity due to any combination of M_1 , M_2 and M_3 can be obtain by the equation:

$$S_p = \left[\frac{0.86 \times 1.95}{h^{2/3}} M_1 + \frac{1.95}{h^{2/3}} M_2 + M_3 \right] \times \frac{1}{Z} \quad (30)$$

Equation (30) is an upper bound because the maximum stress intensities due to M_1 and M_2 do not occur at the same location on the elbow.

The Code gives K_2C_2 for curved pipe as $(1.95/h^{2/3}) \times (1.0)$, but not less than 1.5. Accordingly, the Code equation for maximum stress intensity is:

$$S_p = \frac{1.95}{h^{2/3}} \left(M_1^2 + M_2^2 + M_3^2 \right)^{1/2} \times \frac{1}{Z} \quad (31)$$

If the lower bound on $1.95/h^{2/3}$ were 1.0 rather than 1.5* and if h were ≥ 2.723 , then Equation (31) becomes identical to Equation (27) for straight pipe. A large value of h means that the elbow characteristics are insignificant and the elbow response to moment loadings is the same as for straight pipe.

If h is small, Equation (31) is always conservative. The amount of conservatism depends upon the ratios of the moments M_1 , M_2 and M_3 ; these moments come from the piping systems analysis and the ratios depend upon the specifics of the system and loadings. To illustrate, we take the previously cited example of a 24" ANSI B16.9 elbow with $t = 0.5$ "; $h = 0.130$, $1.95/h^{2/3} = 7.60$:

Relative Magnitudes of Moments			Stress Ratio	
M_1	M_2	M_3	Equation (31)	Code Theory
			Equation (30)	
1	0	0	$1.95/(0.86 \times 1.95)$	$= 1.16$
0	1	0	$1.95/1.95$	$= 1.00$
0	0	1	$7.60/1.00$	$= 7.60$

Accordingly, the Code Equation is always conservative for individual moments; highly so for M_3 by itself.

The theory involved in developing the relationship of Equation (29) is described by Dodge and Moore [17]. However, Reference [17] goes further and investigates the implications of the resultants moment, $(M_1^2 + M_2^2 + M_3^2)^{1/2}$, used in Equation (31). Let us assume, to illustrate the problem, that $M_1 = M_2 = M$ and assume that the stress location and stress direction for M_1 and M_2 are identical. Then Equation (31) gives:

$$S_p = \frac{1.95}{h^{2/3}} (M^2 + M^2)^{1/2} = \frac{1.95}{h^{2/3}} M \times 1.414 \quad (32)$$

* The lower bound of 1.5 was imposed because the ends of elbows are often tapered to provide an adequate dimensional alignment for the weld between elbow and mating product.

However, if, in fact, stresses due to M_1 and M_2 occurred at the same location and direction, S_p would be:

$$S_p = \frac{1.95}{h^{2/3}} (1M + 0.86M) = \frac{1.95}{h^{2/3}} M \times 1.86 \quad (33)$$

Reference [17], using the analytically-known complete stress field, found that Equation [31] is conservative for all combination of M_1 , M_2 , and M_3 . The assumption made above that maximum stresses due to M_1 and M_2 occur at the same location is obviously incorrect and, indeed, are displaced by about 45° around the elbow circumference. It turns out that, for $h < \sim 1.0$, the highest stresses occur for $M_1 = M_3 = 0$, $M \neq 0$; i.e. a pure in-plane moment. This is reflected by Equation (29).

Reference [17] gives a simple approximation formula for the maximum stress intensities index, C_2 , for elbows with $h < \sim 1.0$:

$$C_2 = \frac{1.938}{h^{2/3}} \frac{1 + 0.25 r/R}{1 + 0.939 h^{-4/3} \exp(-\psi^{-1/4})} \quad (34)$$

where $\psi = PR^2/Ert$. Internal pressure reduces stresses due to moment loading. For $\psi = 0$ and $r/R = 1/3$, C_2 is about 8% higher than the value used in the Code.

Stress Indices for Nozzles

A nozzle in a vessel or branch connection in a run pipe is shown in Figure 6(c). There are nine moments acting on the nozzle/vessel; six of which are independent. Accordingly, the loadings are more complex; six moments versus three for elbows, two for straight pipe. Each of the six moments produces a different stress field.

There are two regions in which maximum stress intensities occur. One is the region of intersection between the nozzle and vessel; region I of Figure 6(c). The other is the region of intersection of the branch pipe with the nozzle; region J of Figure 6(c).

If the maximum stress intensity due to each of the six moments were known, an upper bound on the stress intensity due to any combination of the six moments could be obtained by the equation:

$$S_p = \frac{1}{Z_b} (G_1 M_{xn} + G_2 M_{yn} + G_3 M_{zn}) + \frac{1}{Z_v} (G_4 M_{xv} + G_5 M_{yv} + G_6 M_{zv}) \quad (35)$$

where the G_i 's are the normalized stress intensities due to each individual moment. Equation (35) is an upper bound because the maximum stress intensities due to the various moments are not necessarily at the same locations and/or the stress directions are not necessarily such that they directly add for the combined stress intensity.

The Code equation for S_p due to combinations of moments is:

$$S_p = \frac{K_{2b} C_{2b}}{Z_b} \left(M_{xn}^2 + M_{yn}^2 + M_{zn}^2 \right)^{1/2} + \frac{K_{2r} C_{2r}}{Z_v} \left(M_{xv}^2 + M_{yv}^2 + M_{zv}^2 \right)^{1/2} \quad (36)$$

where

$$K_{2b} C_{2b} = (1.0) \times 3(R/T)^{2/3} (r/R)^{1/2} (t/T)(r/r_p); 1.5 \text{ minimum,}$$

$$K_{2r} C_{2r} = (2.0) \times 0.8(R/T)^{2/3} (r/R); 3.0 \text{ minimum.}$$

The remainder of this Chapter consists of an evaluation of the adequacy of Equation (36) and the $K_{2b} C_{2b}$ and $K_{2r} C_{2r}$ indices. This evaluation makes use of calculated stresses for moment loadings, from the CORTES-SA computer program. The models are dimensionally identical to those used for pressure loading basic series; Table 2 herein. Available test data on stresses due to moment loadings are also used in the evaluation.

Moments on Nozzles

Reference [18] gives normalized maximum stress intensities, $\bar{\sigma}$, for the set of models shown in Table 2. Values of $\bar{\sigma}$ for M_{xn} , M_{yn} and M_{zn} are shown in Table 10 under the heading "CORTES, $\bar{\sigma}$ ". These moments were balanced by moments on the left-hand end of the vessel, hence $M_{xn} = M_{xv}$, $M_{yv} = 0$; etc.

The Code equation for $K_{2b}C_{2b}$ is:

$$K_{2b}C_{2b} = (1.0) \times 3(R/T)^{2/3} (r/R)^{1/2} (t/T)(r/r_p) \quad , \quad (37)$$

but not less than 1.5

The background of Equation (37) is explained in detail in Reference [19]. Briefly, the equation was based on test data from 23 models where stresses due to moments were measured; fatigue test data from 8 models; and Bijlaard's [30] analysis for correlation guidance.

Values of $K_{2b}C_{2b}$ are shown in Table 10 under the heading "Code, $K_{2b}C_{2b}$ "; it is appropriate to directly compare these with the results under "CORTES, $\bar{\sigma}$ ". This comparison indicates that Equation (37) is satisfactory in the sense that $K_{2b}C_{2b}$ is essentially equal to or greater than the largest of three values of $\bar{\sigma}$. It is also apparent that Equation (37) can be highly conservative for nozzles like UA and SlA for combinations of moments, M_i , in which M_{xn} is a minor component. The conservatism becomes even greater when one considers the location of the maximum stress intensity; these locations are shown Table 11. In Model SlA, for example, not only is $\bar{\sigma}$ due to M_{zn} , much smaller than $\bar{\sigma}$ due to M_{xn} , but the maximum stress intensities occur at locations that are 90° apart. It might be feasible to break M_i into separate moments and develop a $C_{2b}K_{2b}$ index for each moment. However, for nozzles in water-cooled reactors, where R/T is usually less than ~ 20 and r/R is usually less than ~ 0.16 , the conservatism in using M_i with a single $C_{2b}K_{2b}$ is not excessive.

One significant aspect of Equation (37) concerns the role of "t". The stress intensity is obtained by:

$$\bar{\sigma} = K_{2b}C_{2b} \cdot \frac{M_i}{\pi r^2 t} \quad (38)$$

Noting that $K_{2b}C_{2b}$ is proportional to t , it is apparent that $\bar{\sigma}$ is independent of the thickness of the branch pipe, t . The reason for this can be visualized by looking at Figure 7(a). If t were doubled or halved, it is intuitively apparent that stresses in the intersection region would not change significantly. The contribution of t_n is reflected by the magnitude of r_p in Equation (37). (In subsequent evaluation discussed herein, t_n will be introduced directly into correlation equations.)

The lower bound of $K_{2b}C_{2b} = 1.5$ in Equation (37) was imposed because of stresses at the nozzle-to-pipe junctions; region J in Figure 6(c). As can be seen in Table 10, the lower bound controls for about the same set of models as those models where CORTES results also indicate that $\bar{\sigma}$ occurs in region J; i.e. the astericked entries under "CORTES, $\bar{\sigma}$ " in Table 10.

Moments Through Vessel*

Values of $\bar{\sigma}$ for M_{xv} , M_{yv} and M_{zv} are shown in Table 12 under the heading "CORTES, $\bar{\sigma}$ ". These moments were balanced by moments on the right-hand end of the vessel, hence $M_{xv} = M_{xv2}$, $M_{xn} = 0$, etc.

The Code equation for $K_{2r}C_{2r}$ is:

$$K_{2r}C_{2r} = (2.0) \times 0.8(R/T)^{2/3} (r/R) \quad (39)$$

but not less than 3.0

The background of Equation (39) is explained in Reference [19]. Briefly, the only applicable data available was one test of a 12 x 4, std. wt. Weldolet. This, along with theoretical considerations of a small hole in a cylindrical shell, provided the basis of Equation (39). (Bijlaard's analysis is not applicable to this loading.)

Values of $K_{2r}C_{2r}$ are shown in Table 12 under the heading "Code, $K_{2r}C_{2r}$ "; it is appropriate to directly compare these with the results under

* Ordinarily, pressure vessels do not have significant moments traversing the vessel. This aspect is relevant to piping in which moments traversing the run pipe may be the major cause of stresses at a nozzle (branch connection). We use the words "vessel" and "nozzle" for continuity of nomenclature in previous portions of this report.

"CORTES, $\bar{\sigma}$ ". This comparison indicates that Equation (39) is excessively conservative. The data from CORTES was used to develop the correlation equation:

$$K_{2r} C_{2r} = 2[(R/T)(r/R)(T/t_n)]^{1/4} \quad (40)$$

but not less than 2.65

Equation (40) is proposed for use in the Code to replace Equation (39). The last column of Table 12 shows values of $K_{2r} C_{2r}$ calculated by Equation (40).

Equation (40) was developed as a relatively simple relationship which is reasonably close to or conservative with respect to the highest of $\bar{\sigma}$ due to the three moments; M_{xv} , M_{yv} or M_{zv} . As can be seen in Table 12, it accomplishes that purpose although slightly unconservative for Models SIL, SIM, SIN, and P30E.

Table 14 summarizes the meager available test data on stresses due to moments traversing the vessel. The first line of Table 14 is the one piece of test data available when Equation (39) was developed. The last three lines of Table 14 are models intentionally made with r_1 and r_2 as close to zero as possible. The values of $\bar{\sigma}$ are the authors of Reference [13] extrapolated estimates; maximum measured stresses were substantially below these estimates.

Recommendations for C_2 and K_2

The present indices of $C_{2b} = 3(R/T)^{2/3} (r/R)^{1/2} (t/T) (r/r_p)$, but not less than 1.5 and $K_{2b} = 1.0$ are deemed appropriate and no Code change is recommended.

The present indices of $C_{2r} = 0.8(R/T)^{2/3} (r/R)$, but not less than 1.0 and $K_{2r} = 2.0$ with $C_{2r} K_{2r}$ product not less than 3.0 are deemed to be excessively conservative and should be replaced by:

" $C_{2r} = 1.15 [(R/T)(r/R)(T/t_n)]^{1/4}$, but not less than 1.5

$$K_{2r} = 1.75$$

The product of $C_{2r}K_{2r}$ shall be a minimum of 2.65."

The limitations associated with the Code use of stress indices for nozzles in vessels or piping are discussed in Chapter 5, along with a summary of recommended Code changes.

4. FLEXIBILITY FACTORS

Introduction

Definitions and Significance of Flexibility Factors

Figure 8(a) shows a simple piping system which can be used to illustrate the concepts of flexibility factors. In a piping system analysis, the actual shell-structures consisting of straight pipe, curved pipe and nozzles/branch connections are modeled as one-dimensional beam elements. Masses are assigned to the beam elements (usually at discrete points) to represent weight or inertia effects. Point loads, sometimes as complex functions of time, may be imposed to represent earthquakes or relief valve thrust loadings. Points B and C may tend to move with respect to Point A (e.g. due to thermal expansion of the pipe or vessels at Points A, B or C); these are imposed on the model as displacements of B and/or C with respect to A.

For an accurate piping system analysis, the flexibility (load-displacement relationship) of all elements of the piping system must be known. The analysis then gives an accurate representation of the moments in the piping system for use in stress analysis.

A straight pipe portion, SP, of the piping system is shown in Figure 8(b). The rotation θ_1 of end-B with respect to end-A is:

$$\theta_1 = \frac{1}{EI} \int_0^L M_1 dx \quad (41)$$

Similar simple equations apply for θ_2 due to M_2 and for displacements of end-B with respect to end-A for M_1 and M_2 . For torsional moment M_3 :

$$\theta_3 = \frac{1}{GJ} \int_0^L M_3 dx = \frac{1.3}{EI} \int_0^L M_3 dx \quad (42)$$

where G = shear modulus, J = polar moment of inertia.

The displacement of B with respect to A for θ_3 is zero. These flexibility relationships are used in all piping system analysis. These are "exact" to the extent that E and I are known exactly. Because of variations in pipe dimensions and E, they are normally no closer than about $\pm 5\%$.

A curved pipe portion, CP, of the piping system is shown in Figure 8(c). The curved pipe is included in the model as a one-dimensional curved element with, in this example, a centerline length $R \times \frac{\pi}{2} = L$. However, the rotation θ_2 of end B with respect to end A is:

$$\theta_2 = \frac{k}{EI} \int_0^{\alpha_0} M_2 R d\alpha \quad (43)$$

where k is the flexibility factor for curved pipe, $k = 1.65/h$, $h = tR/r^2$, t = wall thickness, R = bend radius, r = cross section radius. For some curved pipes, the factor k can be significantly greater than unity. For example, the h for a 24" ANSI B16.9 elbow (R = 36") with 0.50" wall thickness is 0.130 and $k = 1.65/0.130 = 12.7$. Accordingly, the rotation θ_2 by end B with respect to end A, for M_2 , is theoretically 12.7 times as much as would occur in straight pipe of the same centerline length. This is represented by the flexibility factor, k. The k for an out-of-plane moment is also 1.65/h. The k for a torsional moment is 1.0; i.e., like straight pipe. As can be seen in Figure 8(c), M_1 is an out-of-plane moment at end-B but becomes a torsional moment at end-A. This leads to more complex moment-rotation and moment-displacement relationships but those relationships are routinely used in piping system analyses. These are "exact" to the extent that E and I_b are known and, more significantly, to the extent that "end effects" are negligible. The theory which leads to $k = 1.65/h$ ignores the effect of whatever is attached to the ends of the curved pipe. This aspect is discussed in Reference [21] and modifications to k to account for "end effects" are presented.

The nozzle (branch connection) in a vessel (run pipe) portion, BC of Figure 8(a), is detailed in Figure 8(d). The flexibility we are concerned with is due to local deformations in the intersection region between the nozzle and the vessel. Unlike straight pipe or elbows, there is no defined length like L or $R\alpha_0$ to integrate over. However, it is quite easy

to introduce a short element at the surface of the run pipe, called S in Figure 8(d), which would have a flexibility that represents the effect of the rotations due to local deformations in the intersection region. In order to obtain a k for branch connections that is a dimensionless number like for elbows, it is convenient to express the flexibility of the spring S as:

$$\theta = k \frac{Md_o}{EI_b} \quad (44)$$

where M is a moment applied to the branch, I_b is the section modulus of the branch pipe. This form not only makes k dimensionless; it gives an indication of the significance of the magnitudes of k. If, for example, the distance from I to B in Figure 8(a) is $20d_o$, and $k = 40$ then the flexibility of the branch connection could significantly change the results from a piping system analysis which assumes $k = 0$ and hence give inaccurate values of the moments everywhere in the piping system. However, if $k = 2$, then the piping system analysis would not be greatly changed from that assuming $k = 0$. These concepts are embodied in NB-3687.5 and are used in this report.

An aspect of flexibility factors is that a "conservative" flexibility factor cannot be defined. In the stress indices previously discussed, a "conservative" index is one which is higher than the true value of the stress index. At first glance, it might appear that a "conservative" flexibility factor is one that is lower than the true value of the flexibility factor. However, use of such a flexibility factor does not assure that the calculated moments everywhere in a piping system will be less than their true values. This occurs even in a static piping system analysis. In a dynamic analysis, use of anything except the true value of the flexibility factor leads to inaccuracies in calculations of natural frequencies of the piping system and hence questionable moments at all locations in the piping system. Accordingly, the best flexibility factor to use is the one closest to the true value. A sensitivity analysis is needed to determine the importance of flexibility factors in specific piping systems.

Determination of k_x and k_z

Figure 8(e) shows an arrangement which has been used for determination of k . The lengths L_1 , L_2 , and L_3 are essentially arbitrary but they must be long enough so that any end restraints do not effect the local distortions in the nozzle-to-vessel intersection region. However, as discussed in more detail later, these lengths must be no longer than needed because if they are too long, accuracy in determination of k will deteriorate. Figure 8(e) represents either a test model or are analytical (e.g. CORTES-SA) model.

A moment M_{xn} is applied to the nozzle and rotation θ_x of end-N with respect to end-V is measured or calculated. This rotation is due to local deformations in the intersection region (which we want k to represent) plus nominal rotations of the run pipe from V to P and the nozzle from S to N. Accordingly, the nominal beam rotations, θ_b , must be subtracted from the total rotation to find the net rotation for spring S. The flexibility factor, which for M_x is identified as k_x , is then

$$k_x = \frac{\theta_x - \theta_b}{M_{xn} d_o / (EI_b)} \quad (45)$$

The same procedure is followed for θ_z due to M_{zn} , giving k_z .

Other Load-Displacement Relationships

The two flexibility factors k_x and k_z are the main subject of the remainder of this chapter. At this point, it is pertinent to discuss other load-displacement relationships e.g. θ_y due to M_{yn} , θ_x between ends V and V_1 due to M_{xv} , etc. Indeed, considering all possible moment-rotation relationships, we end up with a six by six matrix. The main diagonal of the matrix consists of rotations at the ends and in the direction of the applied moments. There are non-zero, off-diagonal relationships; e.g. M_{xn} is applied, this produces a rotation of end- V_1 with respect to end-V. However, previous work, as discussed in Reference [22], has indicated that

the only significant load-displacement relationships are the two quantified by k_x and k_z . For other load displacement relationships, sufficient accuracy is obtained by modeling as indicated in Figure 8(d) with spring S assigned $k = 0$. For moments traversing through the vessel (M_{xv} , M_{yv} , M_{zv}) the moment-rotation relationships are obtained by equations for straight pipe; e.g. Equation (41).

Flexibility Factors From CORTES-SA

The model is shown in Figure 9. Dimensions are shown in Table 2. Displacements at Points 1 through 9 were either specified as zero (boundary conditions) or were calculated for moments M_{xn} and M_{zn} . Points 1 through 9 are on "cap elements". These are elements with effectively infinite stiffness and constrain the ends to rotate in planes. The axial length of the cap elements is 0.5 inch. Accordingly, the nominal length of the nozzle is $(19.5 - D_o/2)$ inch and the nominal moment-loaded length of the vessel is 19.5 inch.

Calculated Rotations

Calculated rotations are obtained by:

$$\theta_{xc} = \frac{Y_2}{(d_i/2)} \quad (46)$$

$$\theta_{zc} = \frac{Y_1 - Y_3}{d_i} + \frac{X_7 - X_9}{D_i} \quad (47)$$

where

Y_2 = displacement of Point 2 (Figure 9) on inside surface in Y-direction, inch.

Y_1 , Y_3 , X_7 , and X_9 are similarly defined.

d_i = inside diameter of nozzle, inch.

D_i = inside diameter of vessel, inch.

For M_{xn} , end-V of the vessel is anchored (displacements in X, Y, and Z-directions at Points 7, 8, and 9 are specified as zero), hence the

rotation θ_x of end-N with respect to end-V is given by Equation (46). For M_{zn} , the boundary conditions are such that both end-N and end-V rotate, hence θ_z is the sum of the two rotations; given by Equation (47).

Beam Rotations

Beam rotations were calculated by:

$$\theta_b = \frac{M}{E} \left(\frac{19.5 - D_o/2}{I_n} + \frac{f \times 19.5}{I_v} \right) \quad (48)$$

where

M = moment applied to nozzle in CORTES calculations, in-lb.

E = modulus of elasticity = 3×10^7 psi, same as in CORTES calculations.

D_o = vessel outside diameter, inch.

I_n = moment of inertia of branch pipe, $(\pi/64)(d_o^4 - d_i^4)$, in⁴.

I_v = moment of inertia of vessel, $(\pi/64)(D_o^4 - D_i^4)$, in⁴.

f = 1.3 for M_x (torsion in run pipe)

1.0 for M_z (bending in run pipe)

Flexibility Factors

The flexibility factors for spring S [Figure 8(d)] were calculated by:

$$k = \frac{\theta_c - \theta_b}{Md_o/EI_b} \quad (49)$$

If θ_c is almost equal to θ_b , high accuracy is required for both θ_c and θ_b . The problem can be illustrated by going through the calculation of k_x for Model S1-N. From Equation (46):

$$\theta_{xc} = \frac{3.966 \times 10^{-4}}{0.4} = 9.915 \times 10^{-4} \text{ radians}$$

From Equation (48):

$$\theta_{xb} = \frac{44.971}{3 \times 10^7} \left(\frac{19.5 - 6}{.02159} + \frac{1.3 \times 19.5}{527.0} \right) = 9.374 \times 10^{-4} \text{ radians}$$

From Equation (49):

$$k_x = \frac{(9.915 - 9.374) \times 10^{-4}}{44.971 \times 0.96 / (3 \times 10^7 \times 0.02159)} = 0.81$$

Now, let us assume that CORTES in the process of calculating displacements from end-N to the outside surface of the vessel (a length of 14 diameters) under-calculates Y_2 such that the true value of Y_2 is 1.05 times the calculated value. Then $\theta_{xc} = 1.05 \times 9.915 \times 10^{-4}$ and $k_x = 1.55$ instead of 0.81. If we assume* that the true value of Y_2 is 0.95 times the calculated value, then $\theta_{xc} = 0.95 \times 9.915 \times 10^{-4}$ and $k_x = 0.07$. Accordingly, for $\pm 5\%$ errors in calculating Y_2 , k_x varies from 1.55 to 0.07.

However, if $\theta_c \gg \theta_b$, a $\pm 5\%$ error in Y_2 produces much smaller variations in k_x . In Model UA, for example, $\theta_{xc} = 3.345 \times 10^{-3}$, $\theta_{xb} = 2.090 \times 10^{-4}$, $k_x = 47.0$. A $\pm 5\%$ variation in Y_2 gives k_x from 49.5 to 44.5.

Values of k_x and k_z are shown in Table 15 under the headings "CORTES". An asterick indicates that the values of k_x or k_z are based on $(\theta_c - \theta_b)/\theta_c$ of less than 0.1.

Correlation Equations

The Code, NB-3687.5, gives flexibility factors for branch connections in piping meeting the requirements of NB-3640 and with branch diameter to run diameter ratio not over one-third. The equations are:

* If we assumed that the true value of Y_2 is 0.94 times the calculated values, then $k_x = -0.08$. A negative value of k would not be unreasonable. Note, for example, that in Model S1N the thickness t_n extends for a length of $0.647 d_o$. If there were no rotation due to distortion of the intersection region, then k_x would be about -0.6 .

$$k_x = 0.27 \left(\frac{D_o}{T_e} \right)^{3/2} \left(\frac{t}{T} \right) \left(\frac{d_o}{D_o} \right) \quad (50)$$

$$k_z = k_x/3 \quad (51)$$

where the symbols are defined as in this report (see Nomenclature), and

$T_e = T$ for branch connections per Figure 2(a), (b),
and (d).

$T_e = T + A/2d_o$ for k_x } For branch connections per
 $T_e = T + A/d_o$ for k_z } Figure 2(c).

A = actual area of reinforcing within the zone of
reinforcement given in NB-3643.3.

The background of Equations (50) and (51) is explained in detail in Reference [22]. Briefly, the equations were based on test data from 15 models with $d_o/D_o \leq 0.42$. Bijlaard's [20] analysis for a load distributed over a rectangular area on a cylindrical shell was used to guide correlation of the test results.

One significant aspect is the role of "t" in Equation (50). The rotation θ is obtained by:

$$\theta = k \frac{Md_o}{EI_b} \cong k \frac{Md_o}{(\pi/8) d_o^3 t} \quad (52)$$

Now with k proportional to t and with I_b approximately proportional to t , the rotation θ is essentially independent of t . This is equivalent to saying that θ for Model UA for a given moment is the same as for Model S1-A with the same moment. This crude approximation was used because Bijlaard's [20] analysis does not depend upon the wall thickness of the nozzle; indeed there is no nozzle in Bijlaard's analysis. Reference [22], with additional data represented by the first seven lines of Table 16, suggested that Equation (50) be revised by inclusion of the factor $(d/2r_p)$, where r_p is the nozzle radius as defined in Figure 2. This recognizes that increasing

t_n with respect to t distributes the load over a greater area on the vessel and does improve correlation with S1-models. However, with the additional data shown in Table 15, improved correlation equations were developed as discussed in the following.

It was noted that when the k 's from Table 15 for a constant D_o/T were plotted against the parameter $[(d_o/D_o)(T/t_n)]^{1/2} t/T$, a straight line was obtained. This is a good approximation for models with $(\theta_c - \theta_b)/\theta_b > \sim 0.5$. It is a poor approximation for models with $(\theta_c - \theta_b)/\theta_b < 0.1$ however, as discussed earlier, such models may be subject to large errors and, in any event, their k 's are small and probably not significant in any credible piping system configuration.

Figures 10 and 11 show $k/\{[(d_o/D_o)(T/t_n)]^{1/2}(t/T)\}$ plotted against D_o/T . (Excluding those models with $(\theta_c - \theta_b)/\theta_b < 0.1$, astericked in the Tables.) Figure 10 indicates k_x is about proportional to $(D_o/T)^{3/2}$ while Figure 11 indicates k_z is about proportioned to (D_o/T) . These plots lead to the correlation equations:

$$k_x = 0.1 \left(\frac{D_o}{T} \right)^{3/2} \left(\frac{d_o}{D_o} \frac{T}{t_n} \right)^{1/2} \frac{t}{T} \quad (53)$$

$$k_z = 0.2 \left(\frac{D_o}{T} \right) \left(\frac{d_o}{D_o} \frac{T}{t_n} \right)^{1/2} \frac{t}{T} \quad (54)$$

Equations (53) and (54) retain t to the first power hence [see Equation (50)], θ is essentially independent of t . The reason for this can be visualized by looking at Figure 7(a). If t were doubled, it is intuitively apparent that the stiffness of the nozzle is not changed significantly. Indeed, Table 16 models have $t = t_n$ and these correlate reasonably well with Table 15 S1 and P30 models. Similarly, it is intuitively apparent that if t is cut in half the stiffness of the nozzle is not changed. Accordingly, it is essential that k be a linear function of t so that θ (for a given moment) will be independent of t . However, this line of reasoning involves the supposition that L_n is sufficiently large

in Figure 2(a) and (b) and the geometry angle θ for Figure 2(c) models is not greater than about 30° . Accordingly, it is recommended that Equations (53) and (54) be limited to use where:

$$L_n \geq 0.5 [(d_i + t_n)t_n]^{1/2} \quad (\text{for S1-models})$$

$$\theta \leq 40^\circ \quad (\text{for P30-models})$$

Values of k_x and k_y by Equations (53) and (54) are shown in Tables 15 and 16 under the headings "Proposed Code". However, data scatter can be best seen in Figures 10 and 11.

In Figure 10, the "worst" point is Model UF with $D_o/T = 12$, $d_o/D_o = 0.08$. The value of $(\theta_c - \theta_b)/\theta_b$ for this model is 0.1223; a bit higher than our arbitrary cut-off of 0.10. If CORTES over-estimated Y_2 by 10%, then the point for Model UF would be in-line with the correlation equation. On the other hand, CORTES results may be indicating that k does not go to zero as d_o/D_o goes to zero. From a shell-theory viewpoint, it seems intuitively reasonable that as d_o/D_o goes to zero, k must go to zero; i.e. a very small nozzle cannot move the massive vessel-wall. However, in a more detailed sense as suggested by Figure 7(b), there may be nozzle rotations due to localized deformations of the vessel wall. In any event, the results indicate that k is small (i.e. < 2.0) and hence of little significance in the analysis of most piping systems.

In Figure 11, the "worst" point is also Model UF. The value of $(\theta_c - \theta_b)/\theta_b$ is 0.1197. Model S1-I with $D_o/T = 42$, $d_o/D_o = 0.16$ is also well above the correlation equation; the value of $(\theta_c - \theta_b)/\theta_b$ is 0.1188. This could be due to small errors in calculation of Y_2 or local effects as illustrated in Figure 7(b). Again, the k 's are small and of minor significance. One test point, a 24 x 4 fabricated model, is also well above the correlation equation. The reason for this is not apparent; it constitutes the one data-point that is significantly different than given by the correlation equation; i.e., $k_z = 17$ by test, $k_z = 5.85$ by Equation (54). The preponderance of the data suggests an error in this test result.

Recommendations for k_x and k_z

The flexibility factor equations now in NB-3687.5 [Equations (50) and (51) herein] should be replaced by Equations (53) and (54) herein.

The limitations associated with the Code use of flexibility factors for nozzles in vessels or piping are discussed in Chapter 5, along with a summary of recommended Code changes.

5. CODE RECOMMENDATIONS

Limitations on Applicability

Correlation equations have been presented in this report which are based on calculated or test data over a certain range of parameters and for the specific configurations shown in Figure 2. These correlation equations must be used with caution beyond the range of parameters used in developing them or for configurations not included in Figure 2. Almost all of the appropriate restrictions are already in the Code; we discuss those and additional restrictions in the following.

Isolation

The correlation equations are deemed to be valid for nozzles which are isolated from any other gross structural discontinuity, and the rules of NB-3338.2(d)(2) and NB-3339.1(d) are intended for this purpose. Footnote (3) to Table NB-3681(a)-1 includes this aspect by reference to NB-3686. This aspect needs to be included in NB-3687.5 (flexibility factors); see later recommendation. (Work currently in progress indicates a need to change the wording of these paragraphs, but for the present we recommend using the existing rule.)

Nozzles in Cylindrical Vessels or Straight Pipe

The correlation equations are applicable only to nozzles in cylindrical shell portions of vessels or straight pipe. They are not applicable, for example, to nozzles in vessel heads or to nozzles in curved pipe. Tables NB-3338.2(c)-1 and NB-3339.7-1, by the sub-title "Nozzles in Cylindrical Shells" covers this aspect. Footnote (3) to Table NB-3681(a)-1 restricts the indices to branch connections in straight pipe. NB-3687.5 (flexibility factors) needs to include this restriction; see later recommendation.

Radial Nozzles

The correlation equations are applicable only to nozzles with axis normal to the vessel or run pipe wall. They are not applicable to "lateral" or "hillside" nozzles. NB-3338.2(d)(1) and NB-3339.1 state that the indices are applicable if the axis of the nozzle is normal to the vessel wall. However, NB-3338.2(d)(1) goes on to give an index for σ_n on the inside surface for nozzles where the axis of the nozzle makes an angle ϕ with the normal to the vessel wall and provided $d_i/D_i < 0.15$. This report does not address the validity of those indices.

Footnote (3) to Table NB-3681(a)-1 limits the indices to branch connections with axis normal to the pipe surface. This restriction needs to be added to NB-3687.5 (flexibility factors); see later recommendation.

Configuration Limitations

The correlation equations were developed for the specific shapes shown in Figure 2. Figure NB-3338.2-2 shows two additional configurations which have a variable inside diameter. This report does not address the validity of the stress indices for such configurations.

There is no Code-specified minimum on dimension L_1 in Figure 2. The correlation equations were developed from calculations where $L_1 = L_n = 0.5[(d_i + t_n)t_n]^{1/2}$, or from test data where L_n extended even further. The question arises: how small can L_n be and still validly use t_n ? The correlation equations are deemed to be valid only if $L_n > 0.5 [d_i + t_n)t_n]^{1/2}$; if L_n is less than the limit, then t rather than t_n should be used in the correlation equations. This is included in our recommendations.

Figure 2(c) shows an angle θ which is limited to 45° in Fig. NB-3338.2-2; not limited in Fig. NB-3686.1-1. The correlation equations, P30 models, are based on calculations and test data in which $\theta \leq 30^\circ$. The correlation equations cannot be defended for θ much greater than 30° and, if $\theta > 30^\circ$, the value of $t_n = t_p + (2/3)X$ in the correlation equation should be based on $\theta = 30^\circ$. This is included in our recommendations.

Reinforcement can be obtained by the area within the fillet radius, r_2 . As a bounding case, all reinforcement could be obtained by using a large fillet radius; in that case r_2/t_n could be much larger than the ratios of r_2/t_n used in developing the correlation equations. The correlation equations are deemed valid for r_2/t_n up to 12; if $r_2/t_n > 12$ than it should be assumed to be 12 in the correlation equations. This is included in our recommendations.

D/T and d/D Limits

The correlation equations are deemed valid for D_m/T (or D_i/T) ≤ 100 , d_i/D_i (or d_m/D_m) ≤ 0.5 . These limits are imposed in NB-3338.2(d)(3). NB-3339.1(f) limits D_i/T to 200, d_i/D_i to 0.33. The results of this report indicate the D_i/T limit should be reduced to 100; the d_i/D_i limit can be increased to 0.5. This is included in our recommendations.

Footnote (3) to Table NB-3681(a)-1, by reference to NB-3686, imposes limits of $D_m/T < 100$, $d_m/D_m < 0.5$.

Recommendation for NB-3338.2(d)(3)*

- (a) Delete the number "0.8" opposite d/\sqrt{DT} under the column headed "Cylinder".
- (b) Add new line:

$$(d/D) \cdot 133 \quad (D/T) \cdot 188 \quad 1.1$$

with the 1.1 in the column headed "Cylinder".

Recommendation for NB-3339.1(f)

- (a) Delete the "0.8 max." opposite d/\sqrt{DT} under the column headed "Nozzles in Cylindrical Vessels".
- (b) Add new line:

$$(d/D) \cdot 133 \quad (D/T) \cdot 188 \quad 1.1 \text{ max}$$

with the 1.1 max in the column headed "Nozzles in Cylindrical Vessels"

* Nomenclature for this and following recommendations is Code nomenclature

Recommendation for NB-3686

Delete entirely. Also delete Figure NB-3686.1.

The reason for this recommendation is that there appears to be little or no use of it. If needed, NB-3600 permits use of NB-3300 and the table of indices remain in NB-3300. However, this report does not address the validity of any of the indices other than the σ -index, longitudinal plane, inside surface of 3.3.

Recommendations for Table NB-3681(a)-1

Footnote (3) of Table NB-3681(a)-1 is tied into "Branch connection per NB-3640" and, by reference to NB-3686, imposes an appropriate set of dimensional limits. With deletion of NB-3686, the limits must be specified elsewhere and footnote (3) is deemed to be an appropriate place. The recommended wording of footnote (3) is as follows:

- (3) Applicable, provided the following limitations are met.
 Symbols are identified in Figure NB-3643.3(a)-1.
- (a) For branch connections in a pipe, the arc distance measured between the centers of adjacent branches along the outside surface of the run pipe is not less than three times the sum of their inside radii in the longitudinal direction, or is not less than two times the sum of their radii along the circumference of the run pipe.
 - (b) The axis of the branch connection is normal to the run pipe surface.
 - (c) $R_m/T < 50$ and $r'_m/R_m < 0.5$.
 - (d) The inside corner radius, r_1 , is between 10% and 50% of T_r .
 - (e) The outer radius, r_2 , is not less than the larger of $T'_b/2$, $(T'_b + y)/2$ [Fig. NB-3643.3(a)-1(c)] or $T_r/2$.

(f) The outer radius, r_3 (Figure NB-3643.3(a)-1) is not less than the larger of:

- (1) $0.002 \theta d_o$
- (2) $2(\sin\theta)^3$ times the offset for the configurations shown in Figures NB-3643.3(a)-1(a) and (b).

[End of Footnote (3)]

Having established dimensional limits by footnote (3), Footnote (7) can be expanded to cover C_1 and K_1 as well as moment loading indices. The recommended form of Footnote (7) is as follows:

$$(7) \quad (a) \quad C_1 = 1.4 \left(\frac{D_m}{T_r} \right)^{0.182} \left(\frac{r_n}{R_m} \right)^{0.367} \left(\frac{T_r}{t_n} \right)^{0.382} \left(\frac{t_n}{r_2} \right)^{0.148}, \quad \text{but not less than 1.2}$$

$$K_1 = 2.0$$

$$(b) \quad B_{2b} = 0.5 C_{2b}, \text{ but not less than 1.0}$$

$$B_{2r} = 0.75 C_{2r}, \text{ but not less than 1.0}$$

$$C_{2b} = 3(R_m/T_r)^{2/3} (r'_m/R_m)^{1/2} (T'_b/T_r) (r'_m/r_p),$$

but not less than 1.5

$$C_{2r} = 1.15 \left[(R_m/T_r) (r'_m/R_m) (T_r/t_n) \right]^{1/4}, \text{ but not less than 1.5}$$

$$K_{2b} = 1.0$$

$$K_{2r} = 1.75, K_{2r} C_{2r} \text{ shall be a minimum of 2.65}$$

(c) Dimensions are identified in Fig. NB-3643.3(a)-1 and:

D_m = mean diameter of run pipe

$$\left. \begin{aligned} t_n &= T_b \text{ if } L_1 \geq 0.5 [(2r_i + T_b) T_b]^{1/2} \\ &= T'_b \text{ if } L_1 < 0.5 [(2r_i + T_b) T_b]^{1/2} \\ &= T'_b + (2/3)y \text{ if } \theta \leq 30^\circ \\ &= T'_b + 0.385L_1 \text{ if } \theta > 30^\circ \\ &= T'_b = T_b \end{aligned} \right\} \begin{array}{l} \text{Fig. NB-3643.3(a)-1(a)} \\ \text{\& (b)} \\ \text{Fig. NB-3643.3(a)-1(c)} \\ \text{Fig. NB-3643.3(a)-1(d)} \end{array}$$

$$(d) \quad r_n = r_i + t_n$$

$$(e) \quad \text{If } r_2/t_n > 12, \text{ use 12 in calculating } C_1$$

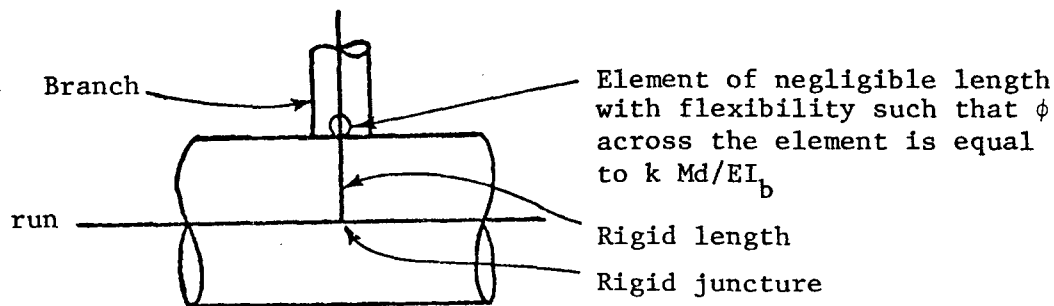
[End of Footnote (7)]

Figure NB-3643.3(a)-1 requires addition of L_1 as shown in Figure 12.

Recommendation for NB-3687.5 (Flexibility Factors)

The recommended wording is as follows:

NB-3687.5 Branch Connections in Straight Pipe. For branch connections in straight pipe meeting the dimensional limitations of footnote 3 of Table NB-3681(a)-1, the load-displacement relationships shall be obtained by modeling the branch connections in the piping system analysis (NB-3672) as shown below.



$$k = 0.1 (D/T_r)^{1.5} [(T_r/t_n)(d/D)]^{1/2} (T'_b/T_r), \text{ for } M_{x3}$$

$$k = 0.2 (D/T_r) [(T_r/t_n)(d/D)]^{1/2} (T'_b/T_r), \text{ for } M_{z3}$$

For other moments see NB-3687.4.

$M = M_{x3}$ or M_{z3} , as defined in footnote (5) of Table NB-3681(a)-1

D = run pipe outside diameter, in.

d = branch pipe outside diameter, in.

I_b = moment of inertia of branch pipe, in⁴. (To be calculated using d and T'_b)

E = modulus of elasticity, psi

T_r = run pipe wall thickness, in.

$$\left. \begin{aligned}
 t_n &= T_b \text{ if } L_1 > 0.5[(2r_i + T_b)T_b]^{1/2} \\
 &= T'_b \text{ if } L_1 < 0.5[(2r_i + T_b)]^{1/2}
 \end{aligned} \right\} \text{ Fig. NB-3643.3(a)-1(a) and (b)}$$

$$\left. \begin{aligned}
 t_n &= T'_b + (2/3)y \quad \text{if } \theta \leq 30^\circ \\
 &= T'_b + 0.385L_1 \quad \text{if } \theta > 30^\circ
 \end{aligned} \right\} \text{ Fig. NB-3643.3(a)-1(c)}$$

$$= T'_b = T_b \left. \right\} \text{ Fig. NB-3643.3(a)-1(d)}$$

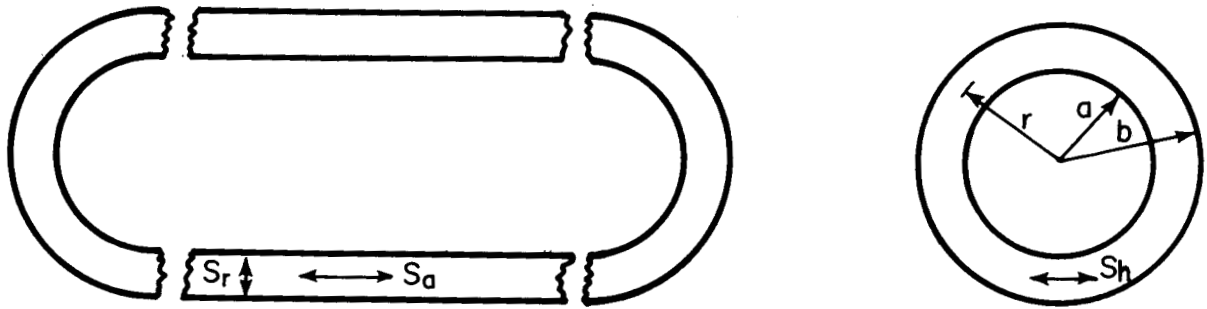
ϕ = rotation in direction of the moment, radians

6. REFERENCES

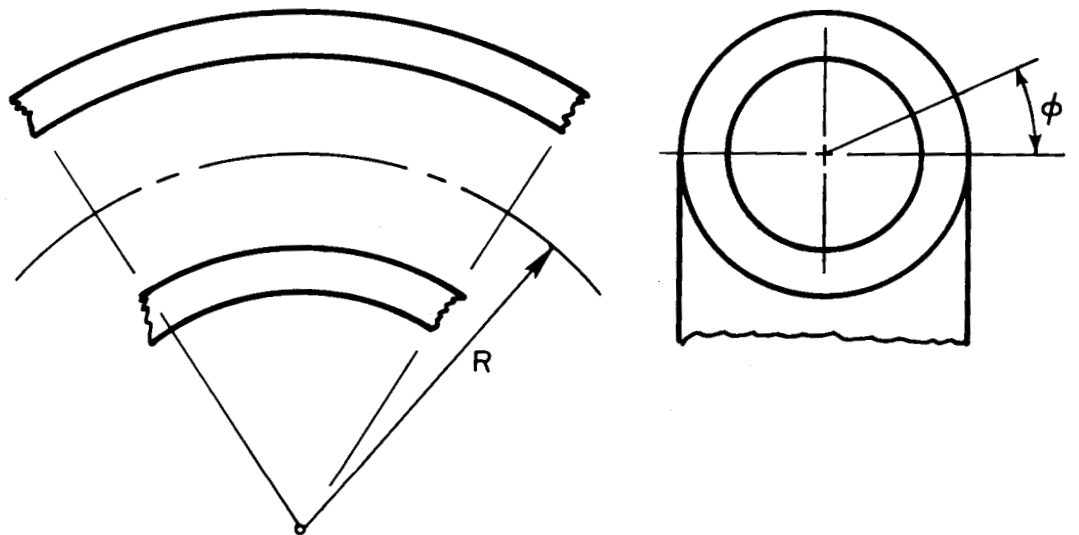
- [1] ANSI (USAS) B31.7-1969, "Nuclear Power Piping". Published by American Society of Mechanical Engineers, 345 East 47th Street, New York, New York 10017 (Obsolete Document, Nuclear Power Piping now covered by ASME Code, Section III).
- [2] Rodabaugh, E. C., "Appropriate Nominal Stresses for Use with ASME Code Pressure-Loading Stress Indices for Nozzles", ORNL/Sub/2913-2, June, 1976, Available from National Technical Information Service (NTIS), 5285 Port Royal Road, Springfield, Virginia 22151.
- [3] Bryson, J. W., Johnson, W. G. and Bass, B. R., "Stresses in Reinforced Nozzle-Cylinder Attachments Under Internal Pressure Loading Analyzed by the Finite-Element Method - A Parameter Study", ORNL/NUREG-4, October, 1977.
- [4] Taylor, C. E. and Lind, N. C., "Photoelastic Study of Stresses Near Openings in Pressure Vessels", Welding Research Council Bulletin No. 113, April, 1966.
- [5] Leven, M. M., "Photoelastic Determination of Stresses in a Reinforced Steam Charging Connection with a Thermal Sleeve", Westinghouse Research Laboratories, Research Report 69-9D7-PHOTO-R1, January 14, 1969.
- [6] Leven, M. M., "Photoelastic Determination of Stresses at an Opening in a Thin-Walled Cylindrical Pressure Vessel", Westinghouse Research Laboratories, Research Report 67-9D7-PHOTO-R1, August 24, 1967.
- [7] Leven, M. M., "Stress Distribution at Two Closely-Spaced Reinforced Openings in a Pressurized Cylinder", Westinghouse Research Laboratories, Research Report 71-9E7-PHOTO-R1, April 9, 1971.
- [8] Seika, M., Isogimi, K. and Inoue, K., "Photoelastic Study of Stresses in a Cylindrical Pressure Vessel with a Nozzle", Bulletin of the JSME, Volume 14, No. 76, 1971.
- [9] Kameoka, T., Sato, E., An, E. and Sato, Y., "Low-Cycle Fatigue of Pressure Vessels with Butt-Welded Nozzles", Proc. First Int'l Conf. on Pressure Vessel Technology, Part II, 1969.
- [10] Pickett, A. G. and Grigory, S. C., "Studies of the Fatigue Strength of Pressure Vessels, Technical Summary Report, Part 1. Cycle Pressure Tests of Full-Size Pressure Vessels", Southwest Research Institute Report to USAEC, September, 1966 (SWRI 1228-1-29).
- [11] Hardenbergh, D. E. Zamrik, S. Y. and Edmondson, A. J., "Experimental Investigation of Stresses in Nozzles in Cylindrical Pressure Vessels", Welding Research Council Bulletin No. 89, July, 1963.

- [12] Hardenbergh, D. E. and Zamrik, S. Y., "Effects of External Loadings on Large Outlets in a Cylindrical Pressure Vessel", Welding Research Council Bulletin No. 96, May, 1964.
- [13] Corum, J. M., Bolt, S. E., Greenstreet, W. L., Gwaltney, R. C. and Bryson, J. W.
- (a) Theoretical and Experimental Stress Analysis of ORNL Thin-Shell Cylinder-to-Cylinder Model No. 1, ORNL-4553, October, 1972.
 - (b) Theoretical and Experimental Stress Analysis of ORNL Thin-Shell Cylinder-to-Cylinder Model No. 3, ORNL-5020, June, 1975.
 - (c) Theoretical and Experimental Stress Analysis of ORNL Thin-Shell Cylinder-to-Cylinder Model No. 4, ORNL-5019, June, 1975.
- Available from NTIS.
- [14] Mershon, J. L., "Preliminary Evaluation of PVRC Photoelastic Test Data on Reinforced Openings in Pressure Vessels", Welding Research Council Bulletin No. 113, April, 1966.
- [15] Truitt, J. B. and Raju, P. P., "Three-Dimensional Versus Axisymmetric Finite-Element Analysis of a Cylindrical Vessel Inlet Nozzle Subject to Internal Pressure--A Comparative Study", ASME Journal of Pressure Vessel Technology, May, 1978.
- [16] Rodabaugh, E. C., Evaluation of C_1 and K_1 Stress Indices for Branch Connections", Westinghouse Electric Corp., WCAP-8858, June 16, 1976.
- [17] Dodge, W. G. and Moore, S. E., "Stress Indices and Flexibility Factors for Moment Loadings on Elbows and Curved Pipe", Welding Research Council Bulletin No. 179, December, 1972.
- [18] Bryson, J. W., Johnson, W. G. and Bass, B. R., "Stresses in Reinforced Nozzle/Cylinder Attachments Under External Loadings Analyzed by the Finite-Element Method - A Parameter Study", ORNL/NUREG-52, To be published.
- [19] Rodabaugh, E. C., "Stress Indices for Small Branch Connections with External Loadings", ORNL-TM-3014, August, 1970, Oak Ridge National Laboratory, Oak Ridge, Tennessee.
- [20] Bijlaard, P. P., "Stresses from Local Loadings in Cylindrical Pressure Vessels", Trans, ASME, August, 1955.
- [21] Rodabaugh, E. C., Iskander, S. K. and Moore, S. E., "End Effects on Elbows Subjected to Moment Loadings", ORNL/Sub-2913/7, March, 1978, Available from NTIS.

- [22] Rodabaugh, E. C. and Moore, S. E., "Flexibility Factors for Small ($d/D < 1/3$) Branch Connections with External Loadings", ORNL/Sub-2913/6. March, 1977, Available from NTIS.
- [23] Jackson, L. R., et. al., "Stresses in Unreinforced Branch Connections", Battelle Memorial Institute, Columbus, Ohio, September 30, 1953.
- [24] Cranch, E. T., "An Experimental Investigation of Stresses in the Neighborhood of Attachments to a Cylindrical Shell, Welding Research Council Bulletin No. 60, May, 1960.
- [25] Pickett, A. G., et. al., "Low Cycle Fatigue Testing of One-Half Scale Model Pressure Vessels", Progress Reports 9 through 12, July, 1964 through January, 1965. Southwest Research Institute, San Antonio, Texas (Contract No, AT(11-1)-1228, U.S. Atomic Energy Commission).
- [26] Mehringer, F. J. and Cooper, W. E., "Experimental Determinations of Stresses in the Vicinity of Pipe Appendages to a Cylindrical Shell", S.E.S.A. Proceedings, Vol. XIV, No. 2.
- [27] Mills, E. J., Atterbury, T. J., and McClure, G. M., "Study of Effects of Cyclic Bending Loads on Performance of Branch Connections, Battelle Memorial Institute, Columbus, Ohio, May, 1962.
- [28] Rodabaugh, E. C. and Moore, S. E., "Phase Report No. 115-10 on Comparisons of Test Data with Code Methods for Fatigue Evaluation", ORNL-TM-3520, Oak Ridge National Laboratory, November, 1971.
- [29] "Criteria of the ASME Boiler and Pressure Vessel Code for Design by Analysis in Sections III and VIII, Division 2", 1969, Published by the American Society of Mechanical Engineers, 345 East 47th Street, New York, New York 10017.
- [30] Pickett, A. G. and Grigory, S. C., "Studies of the Fatigue Strength of Pressure Vessels, Technical Summary Report, Part I, Cyclic Pressure Tests of Full-Size Pressure Vessels", Southwest Research Institute Report to USAEC, September, 1966 (SWRI 12228-1-29).
- [31] Kameoka, Sato, and Sata, "Low-Cycle Fatigue of Pressure Vessels with Butt-Welded Nozzles", Proc. First Int'l Conf. on Pressure Vessel Technology, Part II, Published by the American Society of Mechanical Engineers, 345 East 47th Street, New York, New York 10017.



a. Length of Vessel or Straight Pipe with Closed Ends



b. Portion of Curved Pipe (Closed Ends Remote from Portion Shown)

FIGURE 1. ILLUSTRATION OF CONCEPTS OF STRESS INDICES FOR INTERNAL PRESSURE LOADING OF SIMPLE GEOMETRIES

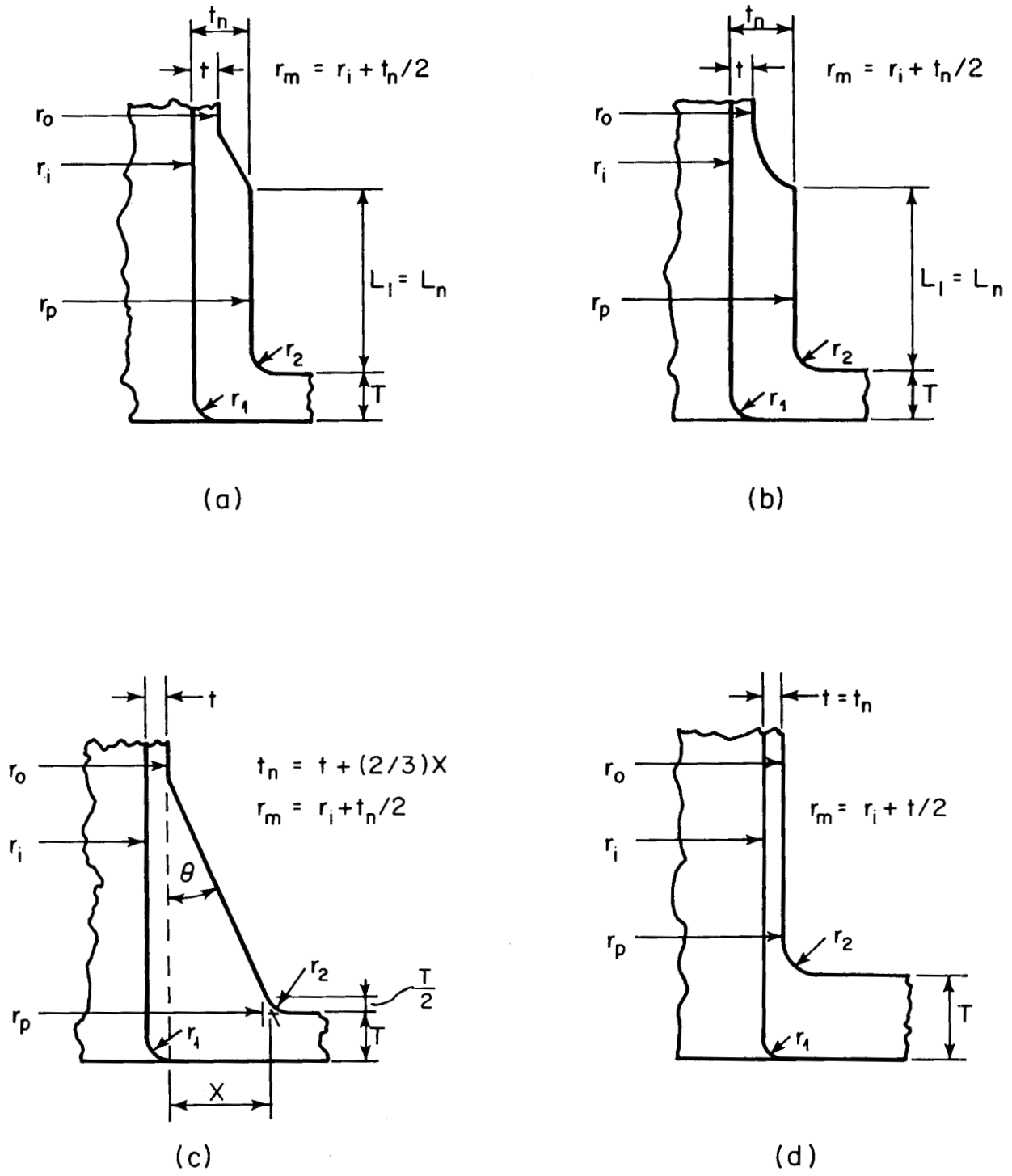


FIGURE 2. NOZZLE CONFIGURATIONS INCLUDED IN THIS REPORT

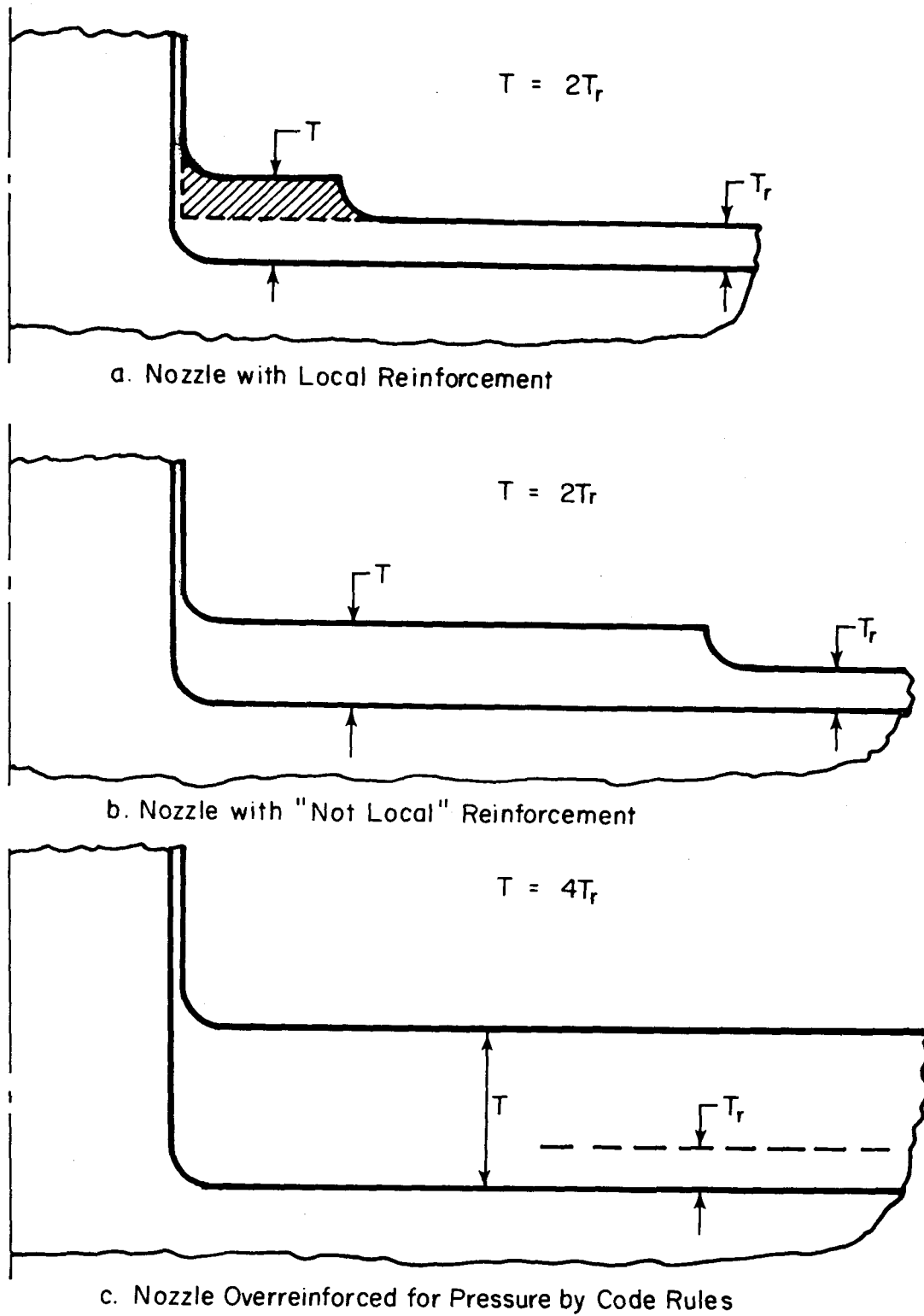
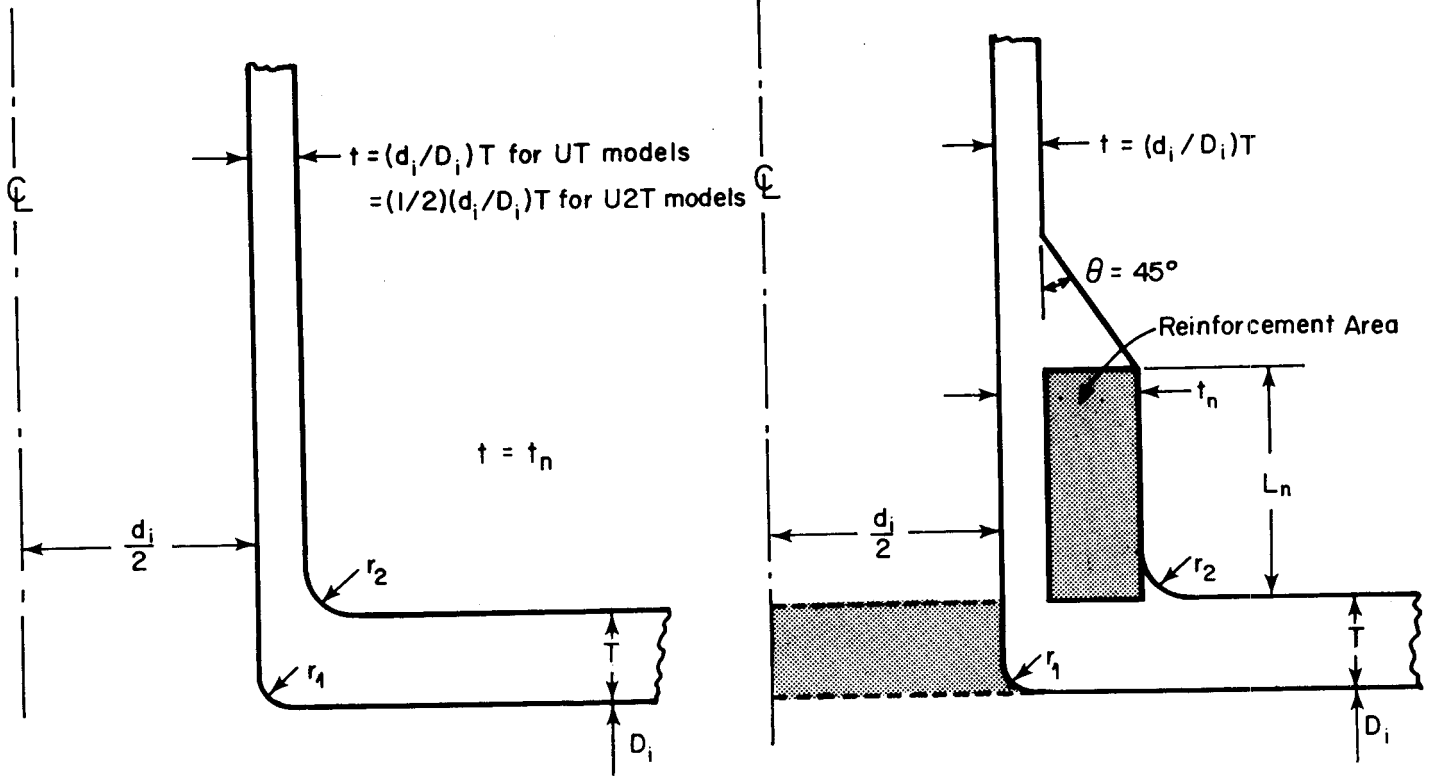
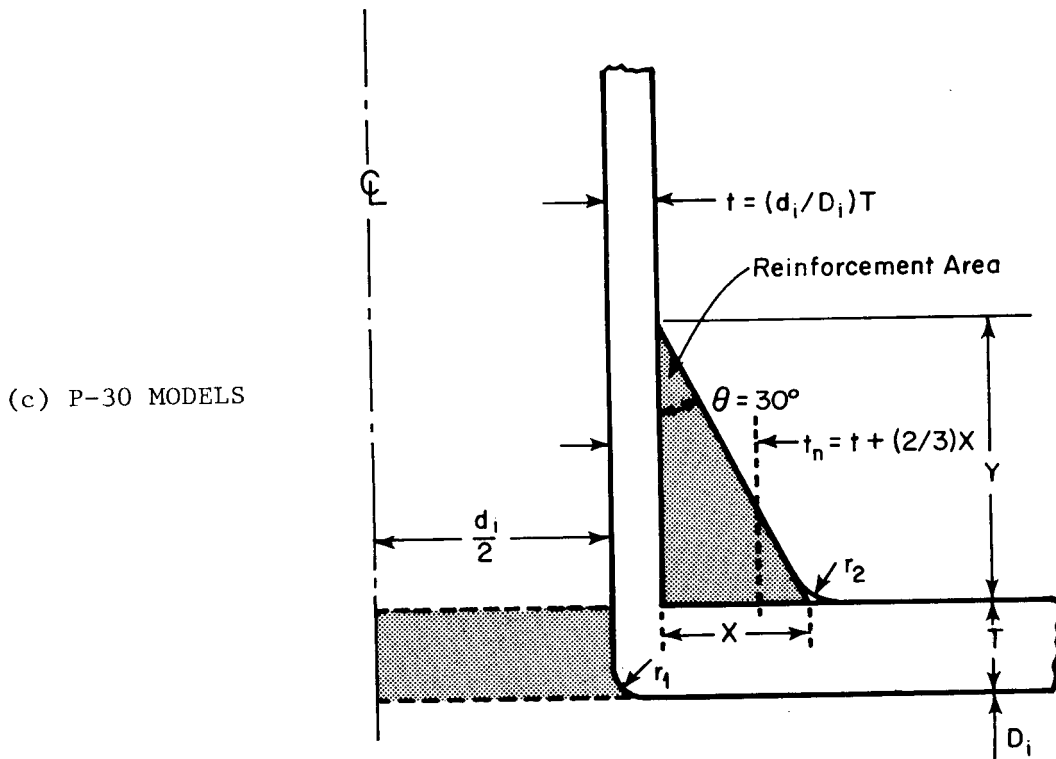


FIGURE 3. ILLUSTRATION OF CONCEPTUAL PROBLEMS IN DEFINING NOMINAL STRESS AS $PD_m/2T$ OR $PD_m/2T_r$



(a) U-MODELS

(b) S-MODELS



(c) P-30 MODELS

FIGURE 4. MODELS USED FOR CALCULATING STRESSES WITH CORTES-SA

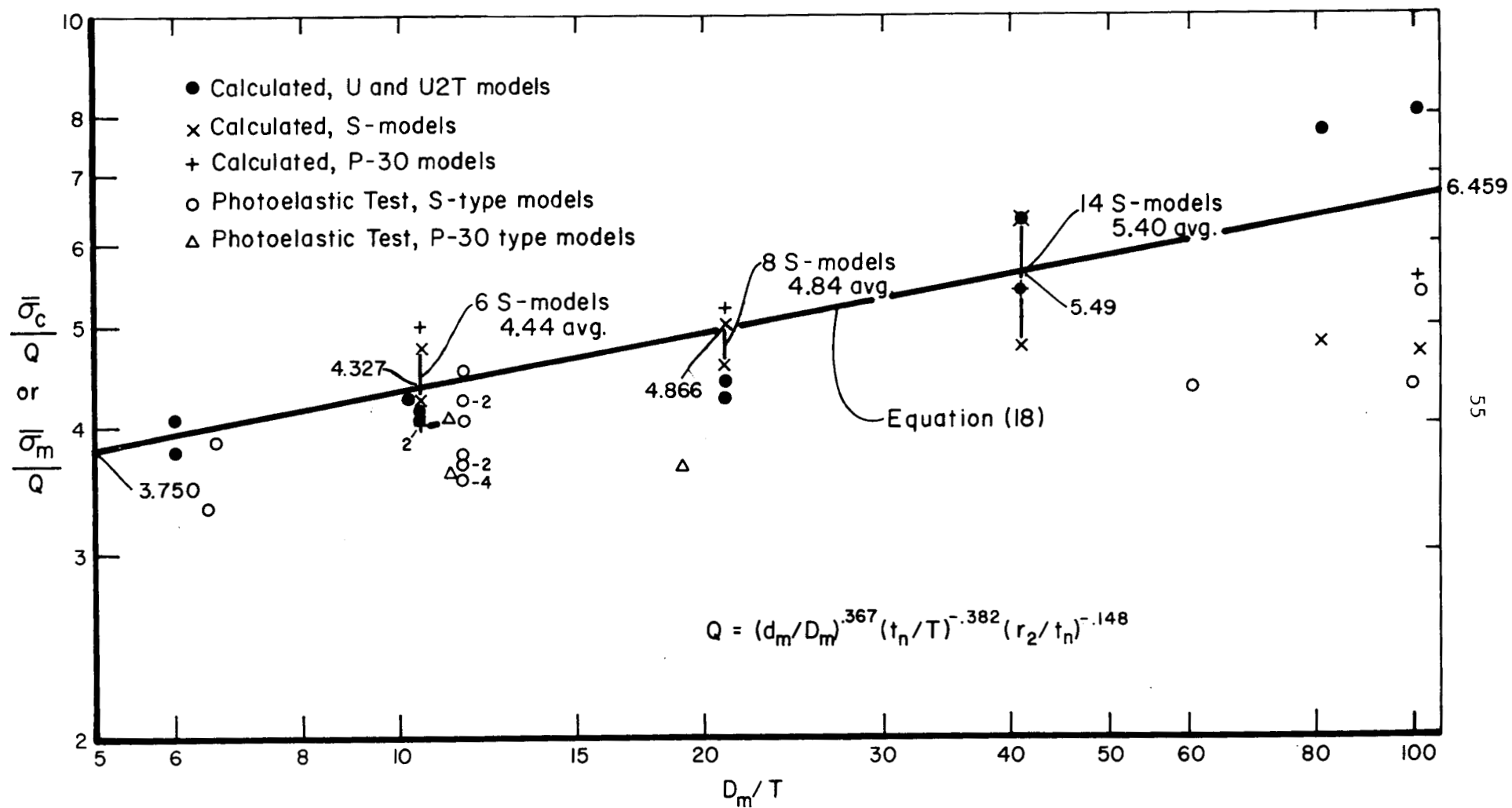


FIGURE 5. COMPARISON OF CORRELATION EQUATION (18) WITH CALCULATED AND TEST MAXIMUM STRESS INTENSITIES

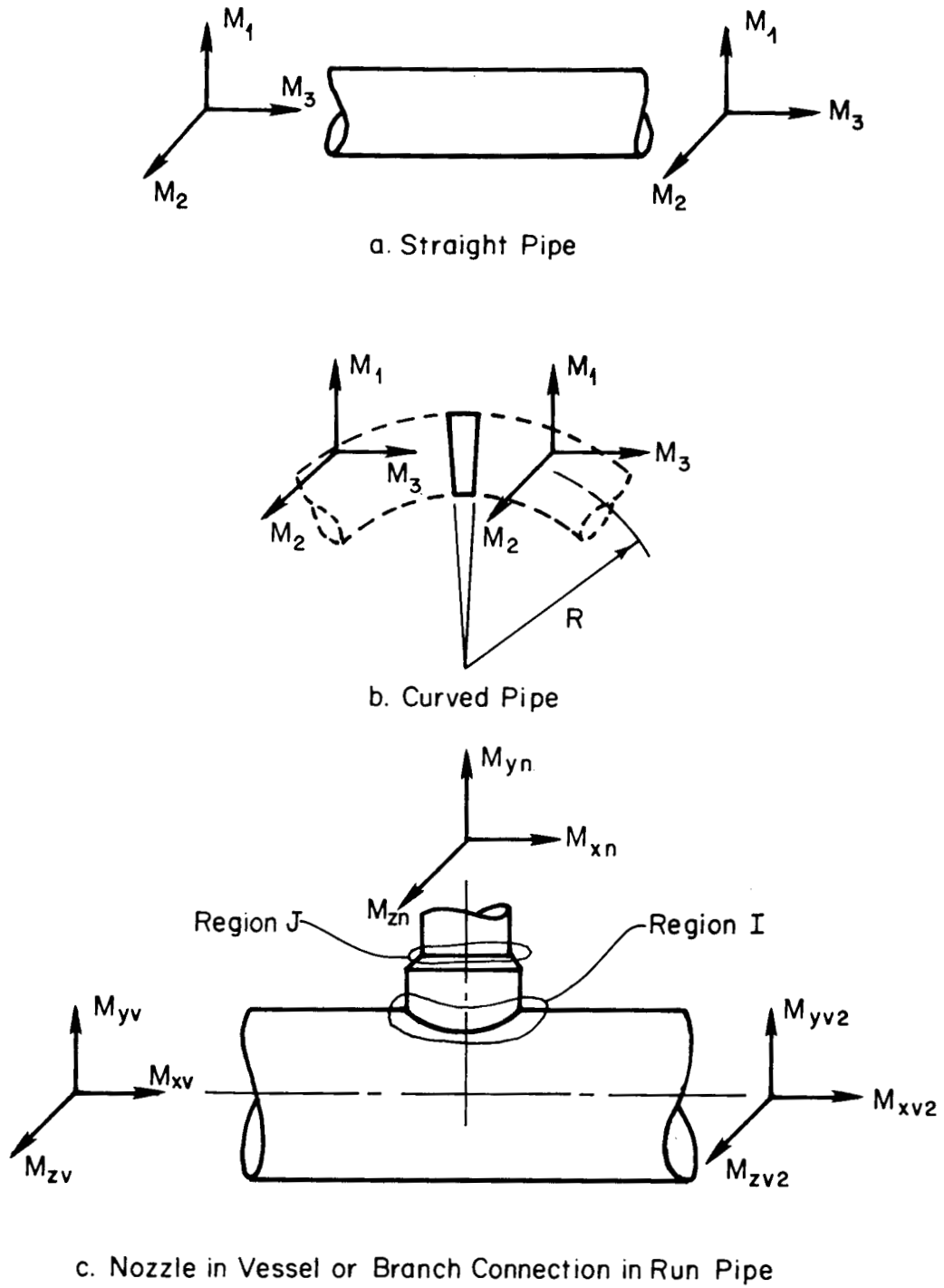
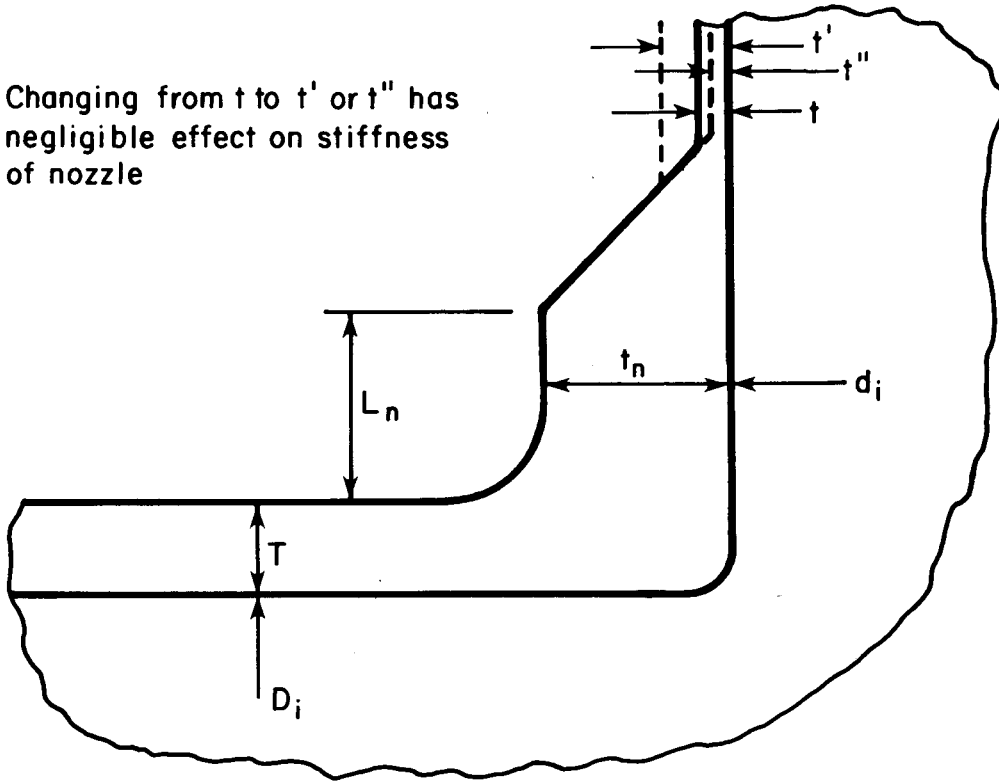
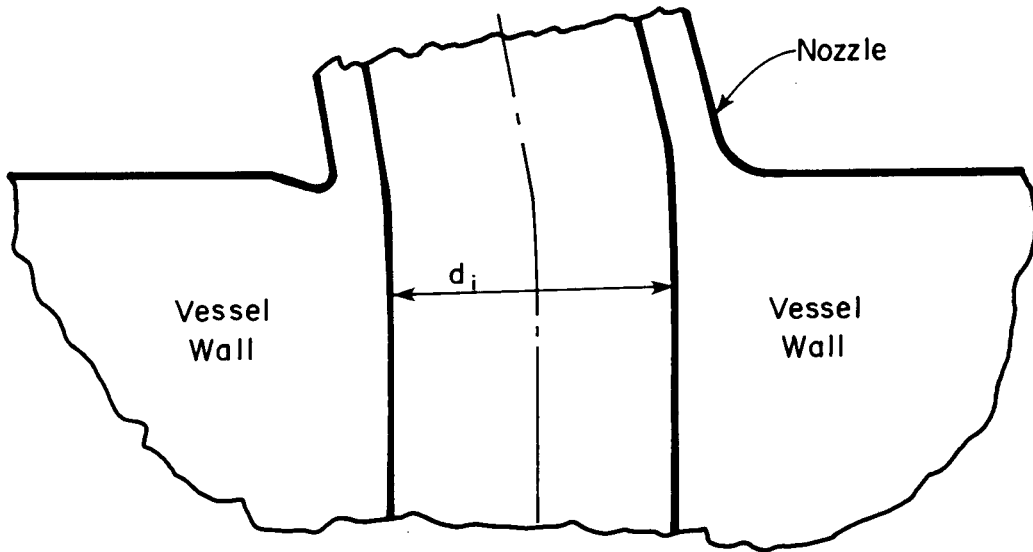


FIGURE 6. ILLUSTRATION OF CONCEPTS OF STRESS INDICES FOR MOMENT LOADINGS

Changing from t to t' or t'' has negligible effect on stiffness of nozzle



a. Illustration of significance of " t " in Equations for $K_{2b}C_{2b}$ and k



b. Illustration of Local Deformation Leading to $k > 0$ for $d_o/D_o \cong 0$

FIGURE 7. ILLUSTRATION OF CONCEPTS OF ROLE OF " t " in $K_{2b}C_{2b}$ AND k AND LOCAL DEFORMATION EFFECTS FOR SMALL d/D

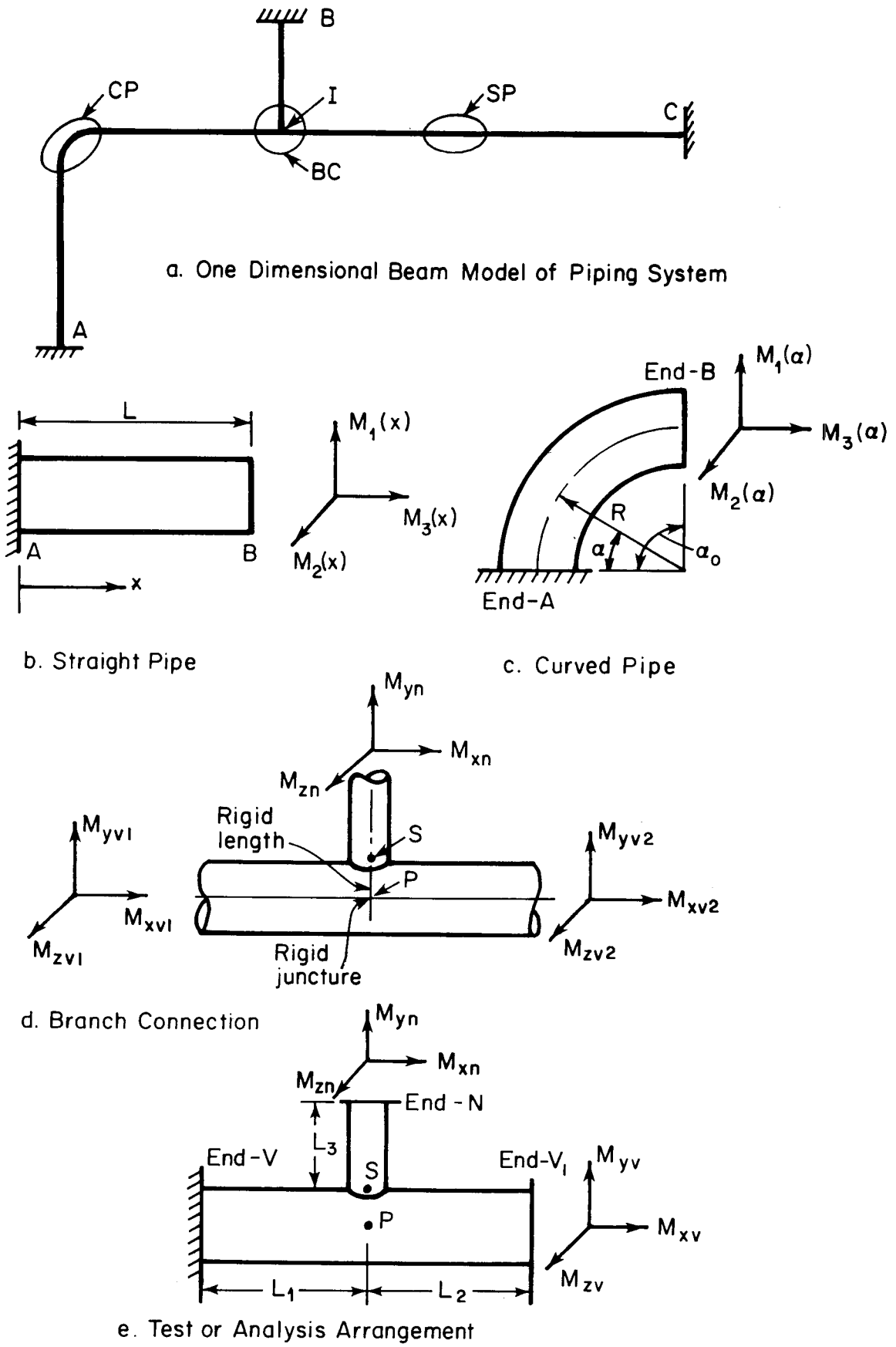


FIGURE 8. ILLUSTRATION OF CONCEPTS OF FLEXIBILITY FACTORS

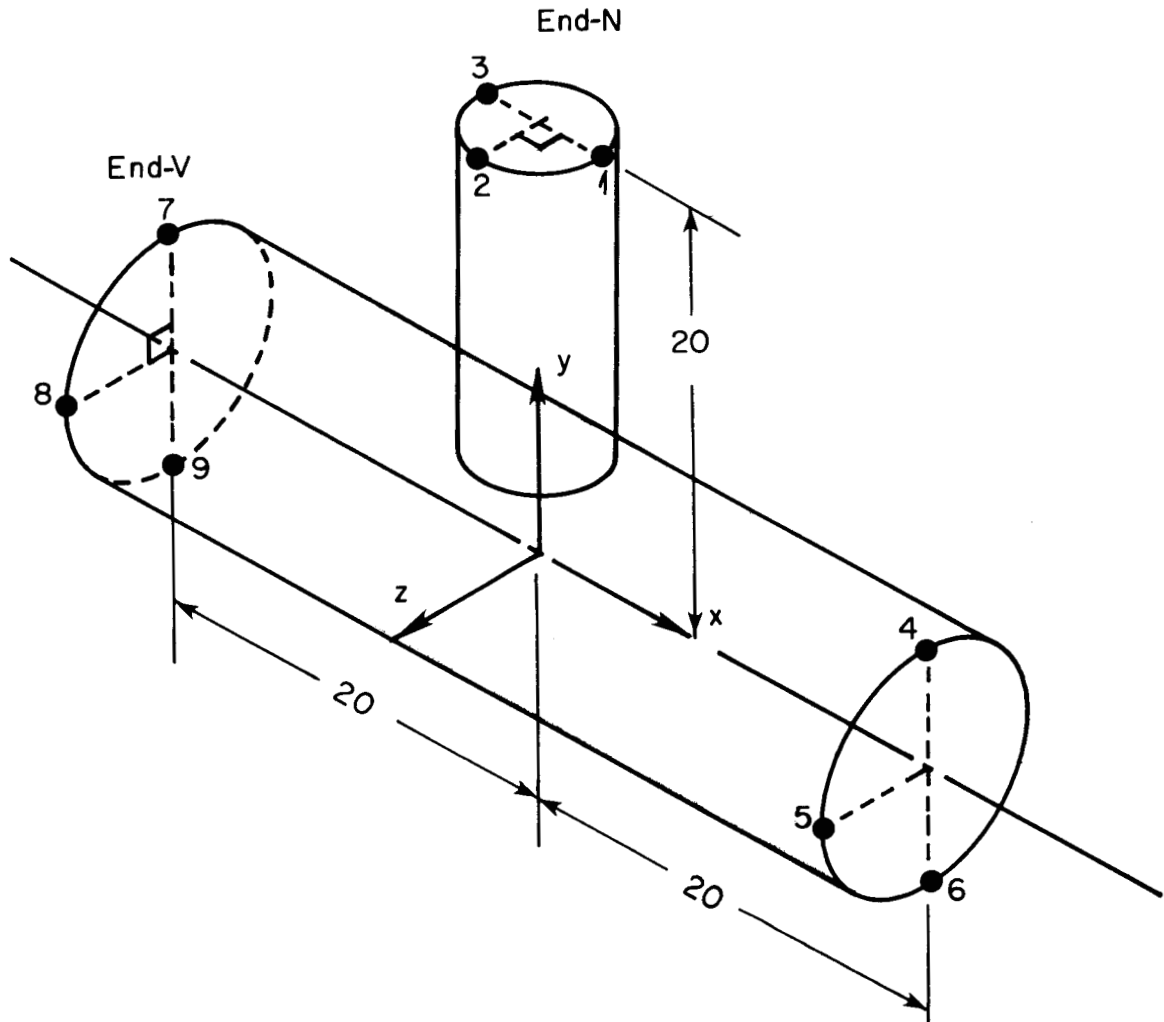


FIGURE 9. CORTES-SA MODEL AND REFERENCE POINTS USED TO OBTAIN FLEXIBILITY FACTORS

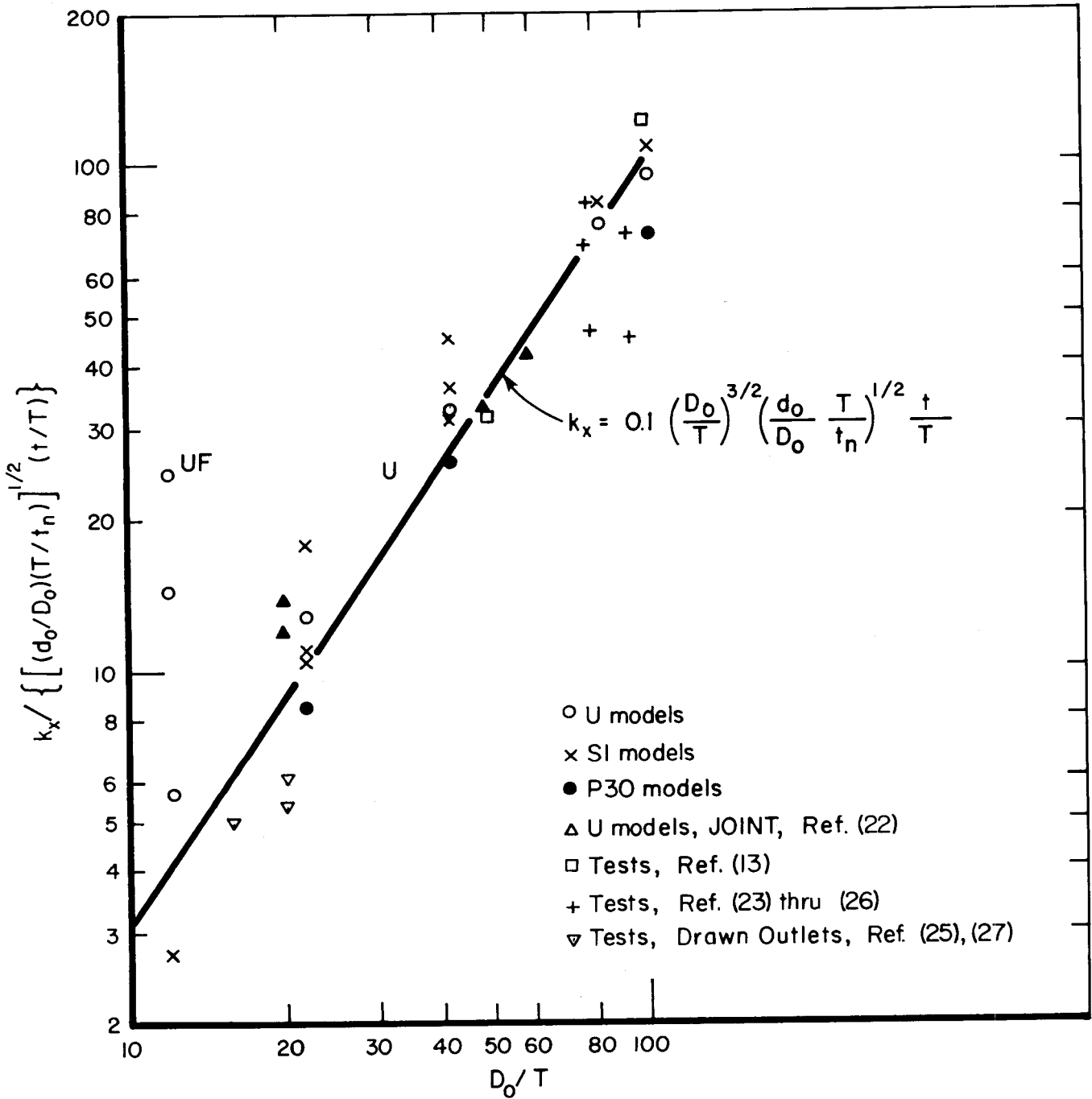


FIGURE 10. COMPARISON OF CORRELATION EQUATION (53) WITH CALCULATED AND TEST-BASED FLEXIBILITY FACTORS, k_x

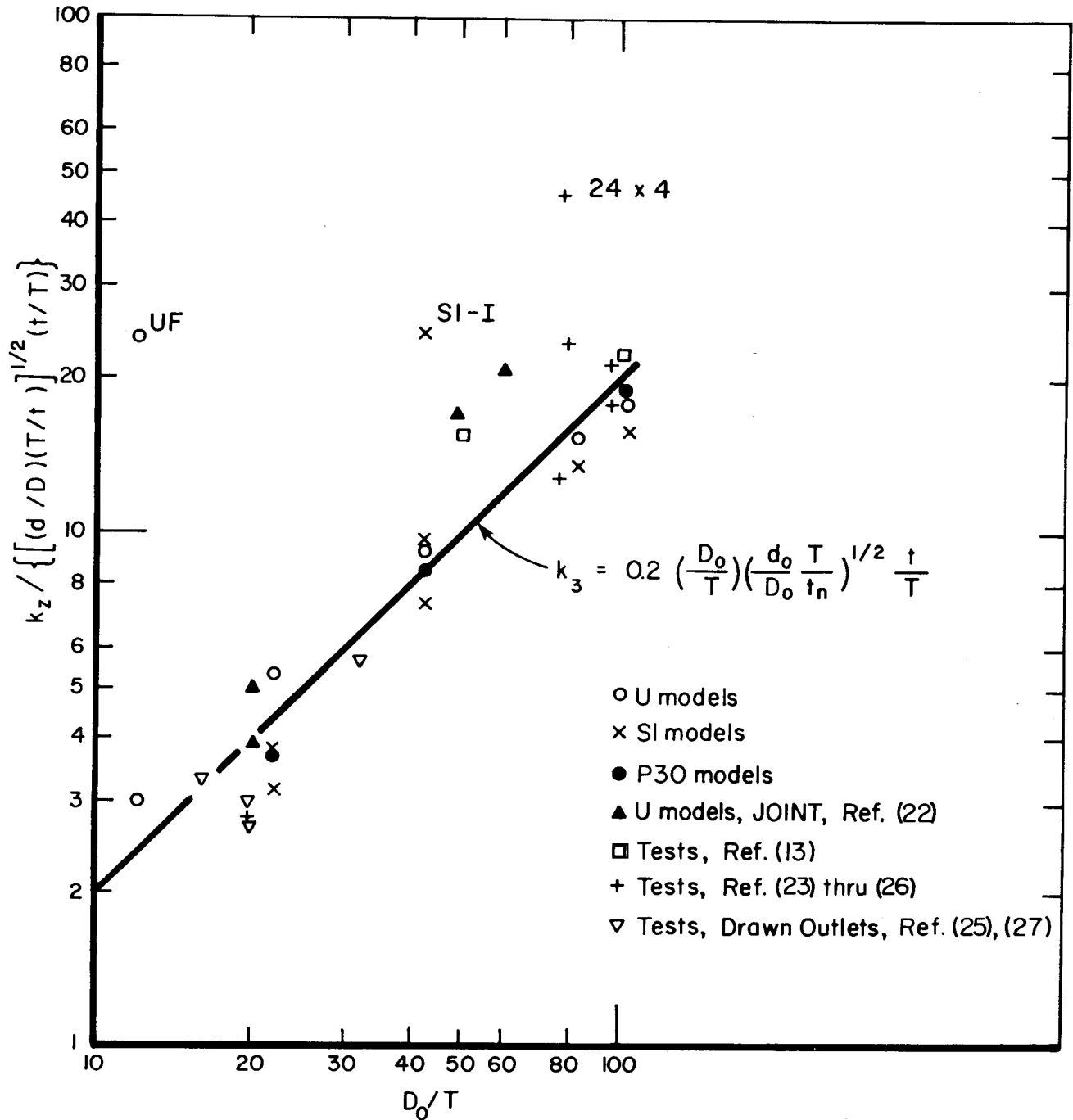
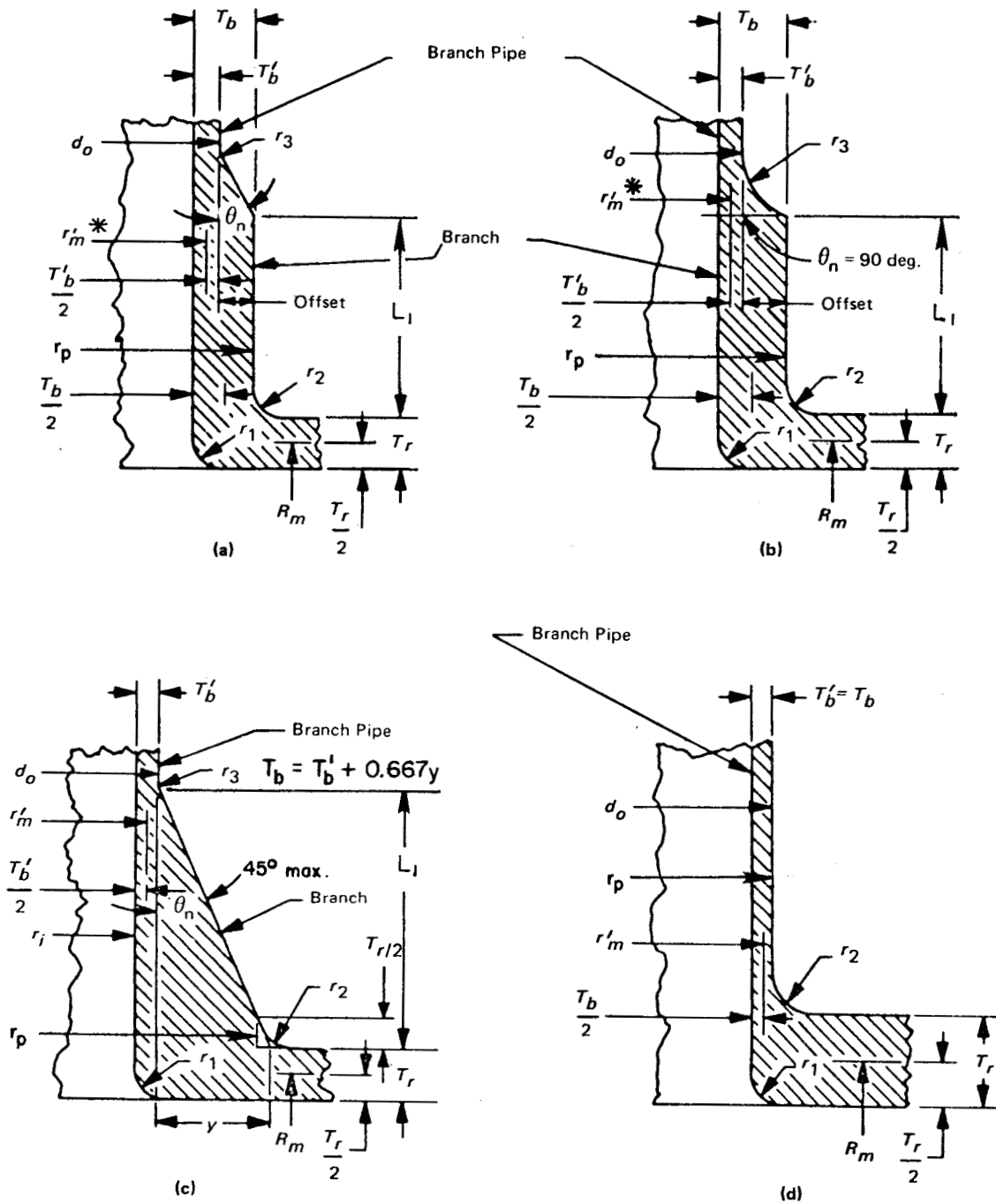


FIGURE 11. COMPARISON OF CORRELATION EQUATION (54) WITH CALCULATED AND TEST-BASED FLEXIBILITY FACTORS, k_z



*NOTE: If L_1 equals or exceeds $0.5 \sqrt{r_1 T_b}$ then r'_m can be taken as the radius to the center of T_b .

FIGURE NB-3643.3(a)-1 BRANCH CONNECTION NOMENCLATURE

FIGURE 12. RECOMMENDED CHANGES TO CODE FIGURE NB-3643.3(a)-1

TABLE 1. STRESS INDICES FOR NOZZLE IN CYLINDRICAL SHELLS, FROM CODE TABLE NB-3338.2(c)-1*

Stress	Longitudinal Plane		Transverse Plane	
	Inside	Outside	Inside	Outside
σ_n	3.1	1.2	1.0	2.1
σ_t	-0.2	1.0	-0.2	2.6
σ_r	$-t_n/R^*$	0	$-t_n/R^*$	0
S	3.3	1.2	1.2	2.6

* Code Table NB-3339.7-1 is identical except that the asterisked entries opposite σ_r are $-2T/(D_i + T)$ which, in conjunction with the specified nominal stress of $(PD_m/2T)$, gives $\sigma_r = -P$ on the inside surface.

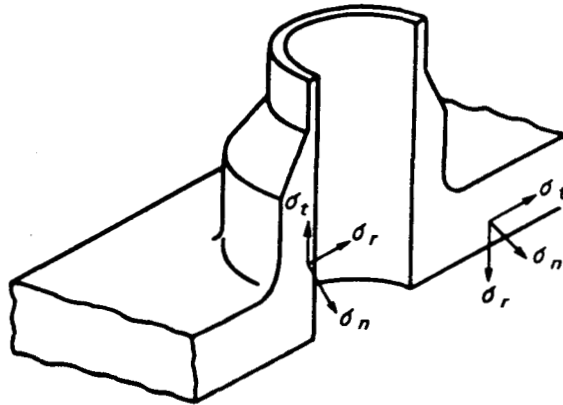


TABLE 2. MAXIMUM STRESS INTENSITIES FROM CORTES-SA ($\bar{\sigma}_c$) AND COMPARISON WITH CORRELATION EQUATION ($\bar{\sigma}_e$), BASIC SERIES OF MODELS FROM REFERENCE [3]

Model	D_m/T	d_m/D_m	t_n/T	r_2/t_n	$\bar{\sigma}_c$ (a)	$\bar{\sigma}_e$ (b)
UA	101	0.500	0.500	1.000	8.14	6.54
B	81	0.500	↓	↓	7.78	6.28
C	41	0.500			5.45	5.55
D	21	0.500			4.26	4.92
E	11	0.500			4.15	4.37
F	11	0.080	0.080	6.250	3.18	3.43
S1A	101	0.538	4.34	0.500	2.38	3.26
B	81	0.543	4.01	↓	2.50	3.24
C	41	0.564	3.14		2.75	3.19
D	21	0.593	2.45		2.95	3.16
E	11	0.629	1.92		3.06	3.15
F	41	0.375	2.56		2.72	2.96
G	21	0.399	1.98		2.83	2.97
H	11	0.429	1.52		2.95	2.99
I	41	0.202	1.88		2.58	2.66
J	21	0.220	1.43		2.67	2.70
K	11	0.244	1.08		2.80	2.77
L	41	0.112	1.38		2.50	2.41
M	21	0.125	1.03		2.59	2.49
N	11	0.138	0.724		2.89	2.63
P30A	101	0.348	3.19		0.500	2.57
B	41	0.364	2.13	0.500	2.84	3.15
C	21	0.381	1.60	0.500	2.89	3.16
D	11	0.402	1.23	0.500	2.92	3.17
E	11	0.121	0.533	0.938	2.96	2.56

(a) Calculated with CORTES-SA.

(b) Correlation Equation (18).

TABLE 3. MAXIMUM STRESS INTENSITIES FROM CORTES-SA ($\bar{\sigma}_c$)
AND COMPARISON WITH CORRELATION EQUATION ($\bar{\sigma}_e$),
AUXILLIARY SERIES OF MODELS

Model	D_m/T	d_m/D_m	t_n/T	r_2/t_n	$\bar{\sigma}_c$ (a)	$\bar{\sigma}_e$ (b)
U2TA	51	0.495	0.250	2.000	8.22	6.77
B	41	0.494	0.250	2.000	7.46	6.50
C	21	0.488	0.250	2.000	5.13	5.73
D	11	0.477	0.250	2.000	4.67	5.05
E	6	0.458	0.250	2.000	4.36	4.46
F	6	0.073	0.040	12.500	3.67	3.50
S75E	11	0.597	1.562	0.613	3.29	3.24
F	41	0.361	2.000	0.640	2.95	3.10
I	41	0.191	1.448	0.649	2.77	2.77
L	41	0.104	1.052	0.653	2.62	2.50
S50D	21	0.546	1.474	0.830	3.42	3.45
F	41	0.347	1.440	0.889	3.17	3.30
G	21	0.359	1.148	0.861	3.25	3.24
I	41	0.181	1.020	0.923	2.96	2.95
J	21	0.190	0.793	0.898	2.94	2.94
L	41	0.096	0.728	0.944	2.72	2.64
M	21	0.103	0.556	0.928	2.77	2.67
S25F	41	0.334	0.880	1.455	3.40	3.65
I	41	0.170	0.588	1.597	3.15	3.28
L	41	0.088	0.404	1.706	2.81	2.94
N	11	0.095	0.241	1.502	3.20	2.95

(a) Calculated with CORTES-SA.

(b) Correlation Equation (18).

TABLE 4. PHOTOELASTIC TEST DATA, NOZZLES IN CYLINDRICAL SHELLS WITH INTERNAL PRESSURE LOADING^(a)

Ref. No.	Iden. (b)	D_m/T	d_m/D_m	t_n/T	r_2/t_n	$\bar{\sigma}_m$ (c)	$\bar{\sigma}_e$ (d)
[4]	C-1A	12.9	.0499	.0478	11.57	2.60	3.30
	C-2A	13.1	.129	.133	4.17	2.94	3.69
	C-3A	12.9	.200	.198	2.79	3.15	3.91
	E-4	13.5	.501	.513	0.889	3.65	4.57
	E-4B	13.2	.500	.503	1.34	3.65	4.32
	E-4E	13.3	.501	.510	1.34	3.89	4.30
	C-3C	6.50	.183	.0910	6.11	3.40	4.03
	C-5C	6.57	.460	.234	2.38	4.46	4.54
	C-5H	13.1	.567	1.38	0.550	2.85	3.50
	E-1	13.2	.289	.514	0.877	3.52	3.73
	E-7	13.4	.289	.513	0.893	3.51	3.73
	E-2	12.9	.288	.490	0.903	3.05	3.76
	E-3	13.0	.288	.496	0.896	3.43	3.75
	F*	19.0	.399	1.818	0.365	2.38	3.15
	P-4A*	12.4	.460	.935	0.571	3.00	3.71
	P-4D*	12.4	.492	1.327	0.402	3.23	3.50
[5]	WC-2AY	60.4	.117	.239	2.512	2.99	4.04
[6]	WC-2AQ	100.1	.129	.139	3.632	3.63**	5.35
[7]	WC-12D	13.2	.160	.547	0.926	2.96	2.92
[7]	WC-100D	102.7	.121	1.234	0.931	2.29	2.80

(a) These results were used in developing correlation Equation (18).

(b) Identification used in cited reference.

(c) Measured, test data.

(d) Correlation Equation (18).

* These are P30-type nozzles, except angle on P-4A is 13.6°

** Maximum stress was on outside surface of pipe at juncture with fillet radius, $\bar{\sigma}_m = 4.75$.

TABLE 5. PHOTOELASTIC TEST DATA FROM SEIKA, ET. AL. [8],
NOZZLES IN CYLINDRICAL SHELLS WITH INTERNAL
PRESSURE LOADING

D_m/T	d_m/D_m	t_n/T	r_2/t_n	$\bar{\sigma}_m$ (a)	$\bar{\sigma}_e$ (b)
17.5	0.10	1.00	0.297	2.2	2.42
17.5	0.12	0.80	0.372	2.3	2.73
17.5	0.13	0.59	0.503	2.5	3.02
17.4	0.10	0.99	0.743	2.0	2.12
17.4	0.12	0.79	0.935	2.2	2.39
17.5	0.13	0.59	1.256	2.4	2.63
17.5	0.10	1.00	1.484	2.0	1.91
17.5	0.12	0.79	1.887	2.2	2.15
17.5	0.13	0.60	2.487	2.3	2.37
16.9	0.31	1.00	0.286	2.8	3.66
16.7	0.33	0.80	0.351	3.0	3.95
17.0	0.34	0.60	0.477	3.1	4.27
16.8	0.31	1.00	0.708	2.6	3.16
16.9	0.32	0.80	0.893	2.8	3.40
16.8	0.34	0.60	1.195	3.0	3.73
16.4	0.31	1.00	1.387	2.6	2.85
16.4	0.32	0.80	1.742	2.8	3.07
16.4	0.33	0.61	2.299	3.0	3.31
17.2	0.49	1.00	0.293	3.1	4.34
17.3	0.50	0.80	0.366	3.4	4.60
17.4	0.51	0.60	0.489	3.6	4.97
17.2	0.49	1.00	0.731	3.0	3.78
17.3	0.50	0.79	0.923	3.2	4.04
17.3	0.51	0.60	1.220	3.4	4.33
16.8	0.48	1.00	1.418	2.9	3.39
16.9	0.49	0.80	1.786	3.2	3.60
16.7	0.50	0.60	2.353	3.4	3.87

(a) Measured, test data.

(b) Correlation Equation (18). Average $\bar{\sigma}_e/\bar{\sigma}_m = 1.187$

TABLE 6. STRAIN GAGE TEST DATA ON STEEL MODELS OF NOZZLES IN CYLINDRICAL SHELLS WITH INTERNAL PRESSURE LOADING

Ref. No.	Iden. (a)	D_m/T	d_m/D_m	t_n/T	r_2/t_n	$\bar{\sigma}_m$ (b)	$\bar{\sigma}_e$ (c)
[9]	F13	23.7	0.188	1.00	0.500	2.63	2.99
	F*13	23.7	0.265	1.00	0.500	2.69	3.38
	F20	15.7	0.284	1.04	0.418	2.80	3.25
[10]	2	19.0	0.315	1.20	0.312	3.02	3.47
	6†	19.0	0.327	1.43	0.524	3.10	3.04
	8	19.0	0.106	0.572	0.309	2.73	3.09
	9†	19.0	0.098	0.361	0.150	2.73	3.98
	11	19.0	0.058	0.094	1.330	2.69	3.98
[11]	M†	19.0	0.6	2.0	1.0††	3.0	3.04
	F†	19.0	0.4	1.4	1.0††	2.6	3.00
	I†	19.0	0.4	1.4	1.0††	2.7	3.00
[12]	R	19.0	0.635	0.687	1.0	5.1	4.67
[13]	ORNL-1	99.0	0.500	0.500	(0.20)**	9.91	8.29
	ORNL-3	49.0	0.114	0.840	(0.060)	4.02	4.15
	ORNL-4	49.0	0.125	0.320	(0.156)	8.13	5.39

(a) Identification used in cited reference.

(b) Measured, test data.

(c) Correlation Equation (18). Average $\bar{\sigma}_e/\bar{\sigma}_m = 1.096$

* Fillet weld, r_2 taken as equal to leg of weld.

† P30-type nozzle.

†† t_n and r_2 estimated from sketches and photographs.

** $r_2 \approx 0.01$ in., see text.

TABLE 7. STRESS INDICES FOR S1-TYPE NOZZLES MEETING
NB-3331 AND NB-3334 RULES

D_i/T	$\bar{\sigma}_e$ for d_i/D_i of:						
	.02	.04	.08	.12	.16	.32	.50
5	2.55*	2.79*	2.52	2.68	2.79	3.04	3.17
10	2.85*	3.13*	2.51	2.67	2.77	3.00	3.15
20	3.20*	2.23	2.48	2.60	2.70	2.97	3.16
40	3.62*	2.21	2.41	2.55	2.65	2.97	3.19
80	1.95	2.13	2.37	2.52	2.64	2.99	3.24
100	1.93	2.12	2.36	2.52	2.64	3.00	3.25

$$\bar{\sigma}_e = 2.8 \left(\frac{D_m}{T} \right)^{.1815} \left(\frac{d_m}{D_m} \right)^{.367} \left(\frac{t_n}{T} \right)^{-.382} \left(\frac{r_2}{t_n} \right)^{-.148} \quad (18)$$

$$\frac{D_m}{T} = \frac{D_i}{T} + 1$$

$$\frac{d_m}{D_m} = \frac{(d_i/D_i)(D_i/T)(T/t_n) + 1}{(D_i/T) + 1} \times \frac{t_n}{T}$$

$$\frac{t_n}{T} = \text{calculated by Equation (14) and (15)}$$

$$\frac{r_2}{t_n} = 0.5 \text{ if } (t_n/T) > 1; = 0.5 T/t_n \text{ if } (t_n/T) < 1.$$

* These are nozzles where $(d_i/D_i) \sqrt{D_i/T} < 0.1414$. No reinforcing is required by Code rules, $t_n/T = d_i/D_i$

TABLE 8. STRESS INDICES FOR SI-TYPE NOZZLES
MEETING NB-3339 RULES

D_i/T	$\bar{\sigma}_e$ for (d_i/D_i) of:						
	.02	.04	.08	.12	.16	.32	.50
5	2.55*	2.79*	2.90	2.86	2.93	3.23	3.33
10	2.85*	3.13*	2.84	2.93	3.04	3.31	3.29
20	3.20*	3.01	2.85	3.01	3.13	3.22	3.20
40	3.62*	2.74	2.91	3.07	3.15	3.12	3.00
80	3.03	2.71	2.97	3.04	3.03	3.00	2.98
100	2.86	2.72	2.99	3.00	2.99	2.95	2.93

$$\bar{\sigma}_e = 2.8 \left(\frac{D_m}{T} \right)^{.1815} \left(\frac{d_m}{D_m} \right)^{.367} \left(\frac{t_n}{T} \right)^{-.382} \left(\frac{r_2}{t_n} \right)^{-.148} \quad (18)$$

$$\frac{D_m}{T} = \frac{D_i}{T} + 1$$

$$\frac{d_m}{D_m} = \frac{(d_i/D_i)(D_i/T)(T/t_n) + 1}{(D_i/T) + 1} \times \frac{t_n}{T}$$

$$\frac{t_n}{T} = \text{calculated by Equation (20)}$$

* These are nozzles where $(d_i/D_i) \sqrt{D_i/T} < 0.1414$. No reinforcing is required by Code rules, $t_n/T = d_i/D_i$.

TABLE 9. STRESS INDICES FOR U2T-TYPE NOZZLES MEETING
NB-3331/3334 AND NB-3339 RULES BY REINFORCE-
MENT IN VESSEL OR RUN PIPE

D_i/T	$\bar{\sigma}_e$ for d_i/D_i of:					
	.02	.04	.08	.16	.32	.50
5	2.55	2.79	3.07	3.36	3.69	* 3.92
10	2.85	3.13	3.43	3.76	4.12	4.37
20	3.20	3.51	3.85	4.23	4.64	4.91
40	3.62	3.97	4.35	4.77	5.23	5.56
80	4.09	4.49	4.92	5.40	5.92	6.28
100	4.26	4.67	5.13	5.62	6.17	6.54

$$\bar{\sigma}_e = 2.8 \left(\frac{D_m}{T} \right)^{.1815} \left(\frac{d_m}{D_m} \right)^{.367} \left(\frac{t_n}{T} \right)^{-.382} \left(\frac{r_2}{t_n} \right)^{-.148} \quad (18)$$

$$\frac{D_m}{T} = \frac{D_i}{T} + 1$$

$$\frac{d_m}{D_m} = \frac{d_i}{D_i}$$

$$\frac{t_n}{T} = \frac{t}{T} = \frac{d_i}{D_i}$$

$$\frac{r_2}{t_n} = 0.5 T/t_n$$

* Nozzles to the left of this line have $(d_i/D_i) \sqrt{D_i/T} < 0.8$

TABLE 10. STRESS INDICES FROM CORTES-SA FOR MOMENT LOADING ON NOZZLE AND COMPARISON WITH CODE CORRELATION EQUATION

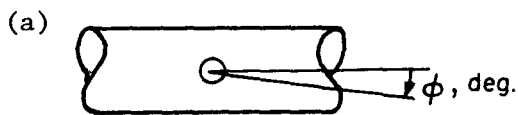
Model	R/T	r/R	t/T	r/r _p	Code K _{2b} C _{2b} (a)	CORTES, $\bar{\sigma}$		
						M _{xn} (b)	M _{yn} (b)	M _{zn} (b)
UA	50.5	0.5	0.5	0.990	14.35	16.60	1.39	7.00
B	40.5	0.5	0.5	0.988	12.36	15.05	1.32	6.54
C	20.5	0.5	0.5	0.976	7.75	10.85	1.25	5.17
D	10.5	0.5	0.5	0.955	4.86	5.77	1.39	3.28
E	5.5	0.5	0.5	0.917	3.03	3.50	1.43	2.64
F	5.5	0.08	0.08	0.917	(1.5)	1.27	1.02*	1.36
S1 A	50.5	0.5	0.5	0.861	12.48	11.07	1.16*	2.19
B	40.5	0.5	0.5	0.843	10.54	9.84	1.16*	2.09
C	20.5	0.5	0.5	0.780	6.20	5.64	1.17*	1.51
D	10.5	0.5	0.5	0.705	3.59	2.81	1.16*	1.42*
E	5.5	0.5	0.5	0.623	2.06	1.56*	1.13*	1.49*
F	20.5	0.32	0.32	0.732	2.98	2.56	1.06*	1.22*
G	10.5	0.32	0.32	0.649	1.69	1.43*	1.07*	1.37*
H	5.5	0.32	0.32	0.563	(1.5)	1.39*	1.05*	1.37*
I	20.5	0.16	0.16	0.646	(1.5)	1.22*	1.02*	1.23*
J	10.5	0.16	0.16	0.555	(1.5)	1.26*	1.02*	1.25*
K	5.5	0.16	0.16	0.468	(1.5)	1.33*	1.03*	1.32*
L	20.5	0.08	0.08	0.551	(1.5)	1.18*	1.01*	1.22*
M	10.5	0.08	0.08	0.459	(1.5)	1.18*	1.01*	1.21*
N	5.5	0.08	0.08	0.391	(1.5)	1.21*	1.02*	1.20*
P30 A	50.5	0.32	0.32	0.808	5.99	3.73	1.08*	1.19*
B	20.5	0.32	0.32	0.743	3.02	1.84	1.08*	1.24*
C	10.5	0.32	0.32	0.695	1.81	1.39*	1.07*	1.32*
D	5.5	0.32	0.32	0.659	(1.5)	1.33*	1.05*	1.35*
E	5.5	0.08	0.08	0.556	(1.5)	1.19*	1.01*	1.20*

(a) $K_{2b} C_{2b} = (1.0) \times 3(R/T)^{2/3} (r/R)^{1/2} (t/T)(r/r_p)$, but not less than 1.5.

(b) Maximum stress intensity ($\bar{\sigma}$) from CORTES. An asterisk in these columns indicates the location of $\bar{\sigma}$ is not in the nozzle-to-vessel intersection region, see Table 11.

TABLE 11. LOCATION OF MAXIMUM STRESS INTENSITY, MOMENT LOADINGS ON NOZZLE

Model	M_{xn} , Out-of-Plane			M_{yn} , Torsion			M_{zn} , In-Plane		
	ϕ (a)	E/J (b)	Surf. (c)	ϕ (a)	E/J (b)	Surf. (c)	ϕ (a)	E/J (b)	Surf. (c)
UA	90	0	out	45	1 N	in	18	1 N	in
B	90	0	out	45	1 N	in	18	1 N	in
C	90	1 N	out	0	1 N	out	9	1 N	out
D	90	0	out	0	1 N	out	9	1 N	out
E	90	0	out	0	1 N	out	0	1 N	out
F	90	3 N	out	90	5 N	out	0	3 N	out
S1 A	90	2 V	out	0	9 N	out	0	1 V	out
B	90	2 V	out	0	7 N	out	0	1 V	out
C	90	1 V	out	0	7 N	out	90	3 V	in
D	90	1 V	out	0	7 N	out	0	7 N	out
E	90	7 N	out	0	7 N	out	0	7 N	out
F	90	1 V	out	0	7 N	out	0	8 N	in
G	90	7 N	out	0	7 N	out	0	7 N	out
H	90	7 N	out	0	7 N	out	0	7 N	out
I	90	7 N	out	0	7 N	out	0	8 N	in
J	90	7 N	out	0	7 N	out	0	7 N	out
K	90	7 N	out	90	7 N	out	0	7 N	out
L	90	9 N	out	0	7 N	out	0	8 N	in
M	90	7 N	out	90	7 N	out	0	9 N	out
N	90	7 N	out	90	7 N	out	0	7 N	out
P30 A	90	3 V	out	0	7 N	out	0	8 N	in
B	90	1 V	out	0	7 N	out	0	8 N	in
C	90	7 N	out	0	7 N	out	0	6 N	out
D	90	7 N	out	0	7 N	out	0	6 N	out
E	90	7 N	out	90	7 N	out	0	7 N	out



(b) E/J \equiv number of elements from
 juncture
 N \equiv on nozzle side of juncture
 V \equiv on vessel side of juncture

(c) in \equiv inside surface
 out \equiv outside surface

TABLE 12. STRESS INDICES FROM CORTES-SA FOR MOMENT LOADING THRU VESSEL AND COMPARISON WITH CODE CORRELATION EQUATION

Model	R/T	r/R	t_n/T	Code $K_{2r} C_{2r}$ (a)	CORTES, $\bar{\sigma}$			Proposed $K_{2r} C_{2r}$ (c)
					M_{xv} (b)	M_{yv} (b)	M_{zv} (b)	
UA	50.5	0.5	0.5	10.93	4.35	1.10	4.62	5.33
B	40.5	0.5	0.5	9.43	4.18	1.09	4.54	5.05
C	20.5	0.5	0.5	5.99	3.53	1.05	4.09	4.26
D	10.5	0.5	0.5	3.84	3.41	1.04	3.60	3.60
E	5.5	0.5	0.5	(3.0)	2.79	1.03	3.17	3.06
F	5.5	0.08	0.08	(3.0)	2.12	1.04	3.11	3.06
SI A	50.5	0.5	4.34	10.93	2.98	1.04	2.19	3.11
B	40.5	0.5	4.01	9.43	2.87	1.04	2.23	3.00
C	20.5	0.5	3.14	5.99	2.43	1.04	2.25	2.69
D	10.5	0.5	2.45	3.84	2.11	1.04	2.07	(2.65)
E	5.5	0.5	1.92	(3.0)	1.70	1.03	2.07	(2.65)
F	20.5	0.32	2.56	3.83	2.01	1.04	2.36	(2.65)
G	10.5	0.32	1.98	(3.0)	1.92	1.04	2.23	(2.65)
H	5.5	0.32	1.52	(3.0)	1.68	1.03	2.08	(2.65)
I	20.5	0.16	1.88	(3.0)	1.81	1.05	2.49	(2.65)
J	10.5	0.16	1.43	(3.0)	1.78	1.04	2.38	(2.65)
K	5.5	0.16	1.08	(3.0)	1.64	1.02	2.33	(2.65)
L	20.5	0.08	1.38	(3.0)	1.76	1.06	2.52	(2.65)
M	10.5	0.08	1.03	(3.0)	1.75	1.04	2.61	(2.65)
N	5.5	0.08	0.72	(3.0)	1.68	1.03	2.63	(2.65)
P30 A	50.5	0.32	3.19	7.00	2.30	1.03	2.24	3.00
B	20.5	0.32	2.13	3.84	2.13	1.04	2.39	2.65
C	10.5	0.32	1.60	(3.0)	1.97	1.03	2.27	(2.65)
D	5.5	0.32	1.23	(3.0)	1.73	1.03	2.05	(2.65)
E	5.5	0.08	0.533	(3.0)	1.72	1.03	2.68	(2.65)

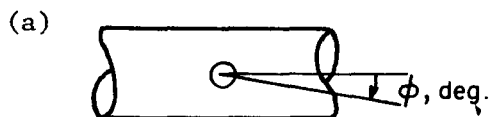
(a) $K_{2r} C_{2r} = (2.0) \times 0.8 (R/T)^{2/3} (r/R)$, but not less than 3.0.

(b) Maximum stress intensity ($\bar{\sigma}$) from CORTES. See Table 13 for locations.

(c) $K_{2r} C_{2r} = 2[(R/T)(r/R)(T/t_n)]^{1/4}$, but not less than 2.65.

TABLE 13. LOCATION AT MAXIMUM STRESS INTENSITY, MOMENT LOADING THRU VESSEL

Model	M_{xv} , Torsion			M_{yv} , In-Plane			M_{zv} , Out-of-Plane		
	ϕ (a)	E/J (b)	Surf. (c)	ϕ (a)	E/J (b)	Surf. (c)	ϕ (a)	E/J (b)	Surf. (c)
UA	54	0	in	90	0	in	90	0	in
B	54	0	in	90	0	in	90	0	in
C	54	0	in	90	0	in	90	0	in
D	54	0	in	(d)	(d)	out	90	0	in
E	54	0	in	↓	↓	out	90	1 N	in
F	45	1 N	in	↓	↓	out	90	1 N	in
S1 A	90	1 V	out	(d)	(d)	out	90	0	in
B	90	1 V	out	↓	↓	out	90	0	in
C	90	1 V	out	↓	↓	out	90	0	in
D	90	1 V	out	↓	↓	out	90	0	in
E	90	1 V	out	↓	↓	out	0	2 V	out
F	90	1 V	out	↓	↓	out	90	0	in
G	45	1 N	in	↓	↓	out	90	0	in
H	45	1 N	in	↓	↓	out	90	1 N	in
I	45	1 N	in	↓	↓	out	90	0	in
J	45	1 N	in	↓	↓	out	90	1 N	in
K	45	1 N	in	↓	↓	out	90	1 N	in
L	45	1 N	in	↓	↓	out	90	0	in
M	45	1 N	in	↓	↓	out	90	1 N	in
N	45	1 N	in	↓	↓	out	90	1 N	in
P30 A	0	1 V	out	(d)	(d)	out	90	0	in
B	36	0	in	↓	↓	out	90	0	in
C	45	1 N	in	↓	↓	out	90	0	in
D	0	1 V	out	↓	↓	out	90	1 N	in
E	45	1 N	in	↓	↓	out	90	1 N	in



(b) E/J \equiv number of elements from juncture
 N \equiv on nozzle side of juncture
 V \equiv on vessel side of juncture

(c) in \equiv inside surface
 out \equiv outside surface

(d) Stress occurs in run pipe, 90° from nozzle axis.

TABLE 14. TEST DATA ON STRESSES FOR MOMENT LOADING THROUGH VESSEL AND COMPARISON WITH CORRELATION EQUATION (40)

Ref. No.	Iden. (a)	R/T	r/R	t_n/T	Test Data, $\bar{\sigma}$			Eq. (40) $K_{2r} C_{2r}$
					M_{xv}	M_{yv}	M_{zv}	
[19]	Weldolet	12.25	0.35	2.11	2.15	0.62	2.09	2.38
[13]*	1	49.5	0.50	0.50	5.0	2.3	3.8	5.30
	3	24.5	0.84	0.84	1.2	1.2	3.2	2.70
	4	24.5	0.32	0.36	1.2	1.3	4.0	3.57

(a) Identification used in cited reference.

* Models with r_1 and r_2 essentially equal to zero. $\bar{\sigma}_m$ values are those extrapolated by the authors of Reference [13]. Maximum measured values are lower than the tabulated values.

TABLE 15. FLEXIBILITY FACTORS FROM CORTES-SA AND COMPARISON WITH PRESENT AND PROPOSED CODE CORRELATION EQUATION

Model	D_o/T	d_o/D_o and t/T	t_n/T	k_x , Out-of-Plane			k_z , In-Plane		
				CORTES (a)	Present Code (b)	Proposed Code (c)	CORTES (a)	Present Code (d)	Proposed Code (e)
UA	102	0.5	0.5	47.0	69.5	51.5	8.89	23.2	10.2
B	82	0.5	0.5	37.2	50.1	37.1	7.68	16.7	8.2
C	42	0.5	0.5	16.2	18.4	13.6	4.58	6.12	6.2
D	22	0.5	0.5	6.92	6.97	5.16	2.65	2.32	4.2
E	12	0.5	0.5	2.84	2.81	2.08	1.50	0.94	1.2
F	12	0.08	0.08	1.96	0.07	0.33	1.91	0.02	0.19
S1 A	102	0.5	4.34	17.8	69.5	17.5	2.70	23.2	3.46
B	82	0.5	4.01	14.5	50.1	13.1	2.42	16.7	2.90
C	42	0.5	3.14	6.32	18.4	5.43	1.46	6.12	1.68
D	22	0.5	2.45	2.33	6.97	2.33	0.72	2.32	0.99
E	12	0.5	1.92	0.69	2.81	1.06	0.24*	0.02	0.61
F	42	0.32	2.56	4.07	7.53	3.08	1.09	2.51	0.95
G	22	0.32	1.98	1.41	2.85	1.32	0.49	0.95	0.57
H	12	0.32	1.52	0.33*	1.15	0.61	0.07*	0.38	0.35
I	42	0.16	1.88	2.11	1.88	1.27	1.14	0.63	0.39
J	22	0.16	1.43	0.95	0.71	0.55	0.71*	0.24	0.24
K	12	0.16	1.08	0.35*	0.29	0.26	0.28*	0.10	0.15
L	42	0.08	1.38	2.02*	0.47	0.52	1.85*	0.16	0.16
M	22	0.08	1.03	1.43*	0.18	0.23	1.39*	0.06	0.10
N	12	0.08	0.72	0.81*	0.07	0.11	0.80*	0.02	0.06
P30 A	102	0.32	3.19	6.91	17.8	10.44	1.89	4.14	2.07
B	42	0.32	2.13	3.20	4.97	3.38	1.07	1.20	1.04
C	22	0.32	1.60	1.20	1.97	1.48	0.54	0.49	0.63
D	12	0.32	1.23	0.33*	0.83	0.68	0.17*	0.21	0.39
E	12	0.08	0.53	0.99*	0.06	0.13	0.98*	0.01	0.07

(a) Values with asterisk are based on $(\theta_c - \theta_b)/\theta_c$ less than 0.1

(b) Equation (50)

(c) Equation (53)

(d) Equation (51)

(e) Equation (54)

TABLE 16. FLEXIBILITY FACTORS FROM JOINT OR TEST DATA AND COMPARISONS WITH PRESENT AND PROPOSED CODE CORRELATION EQUATIONS

Ref. No.	Model (a)	D_o/T	d_o/D_o	t_n/T	k_x , Out-of-Plane			k_z , In-Plane		
					JOINT or Test	Present Code	Proposed Code	JOINT or Test	Present Code	Proposed Code
[22]	11*	59.5	0.115	0.238	6.92	3.39	10.1	3.99	1.13	1.96
"	22*	20.0	0.020	0.020	0.00	0.01	0.82	0.00	0.00	0.08
"	33*	20.0	0.080	0.474	0.96	0.92	1.64	0.75	0.31	0.78
"	44*	20.0	0.320	1.000	7.75	7.73	3.29	2.81	2.58	2.26
"	3*	49.0	0.114	0.840	10.1	8.87	7.53	5.26	2.96	3.03
[13]	1	100	0.500	0.500	60.	67.5	46.0	11.2	22.5	10.0
"	4	50	0.129	0.320	6.4	3.94	8.25	3.1	1.31	2.03
[23]	24 x 4	77	0.19	0.76	31.	26.3	19.1	17.	8.78	5.85
"	24 x 12	77	0.53	0.80	44.	77.4	32.0	8.4	25.8	10.0
[24]	48 x 6	79	0.13	0.45	11.	11.1	16.5	5.6	3.97	3.82
[25]	20 x 12	20	0.64	0.69	--	10.7	4.65	1.8	3.55	2.66
[26]	36 x 4	94	0.12	0.42	10.	12.4	20.5	4.	4.13	4.22
"	36 x 6	94	0.19	0.75	27.	35.1	25.8	8.	11.7	7.10
[27]	16 x 6	32	0.41	0.56	11.8	11.2	7.53	2.7	3.74	3.07
"	16 x 6	16	0.41	0.28	1.7	1.98	2.66	1.1	0.66	1.08
[28]	20 x 6	20	0.33	0.43	2.3	3.43	3.34	1.1	1.14	1.51
"	20 x 12	20	0.64	0.69	3.5	10.7	4.65	1.8	3.55	2.66

(a) Models with asterisk were calculated using the computer program JOINT. Other models are test data.

Reference [13]: Machined models with r_1 and $r_2 \approx 0$

Follow group of six models: Like U-type models except with fillet welds

Last group of four models: drawn outlet tees with crotch contour as sketched

